

Challenging Image analysis problems in the exploitation of **hyper**-spectral remote sensing data for the visible and infrared spectral region

Christoph Borel, PhD

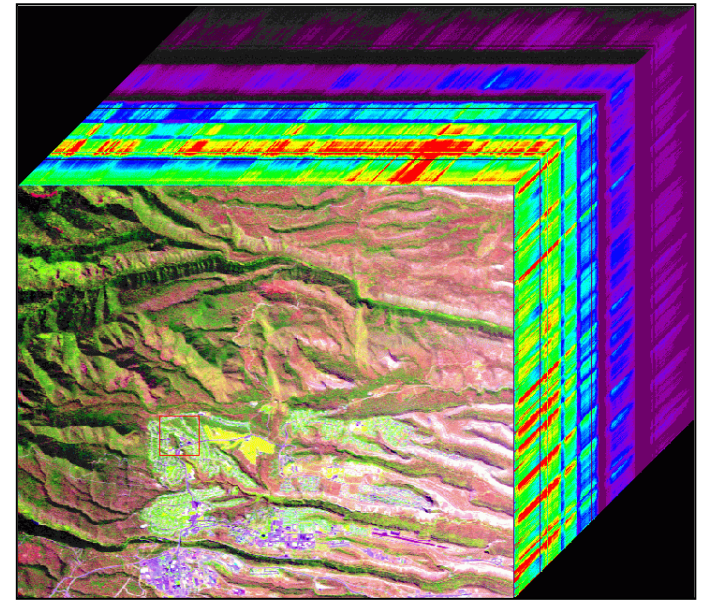
Los Alamos National Laboratory

cborel@lanl.gov

<http://nis-www.lanl.gov/~borel>

Content:

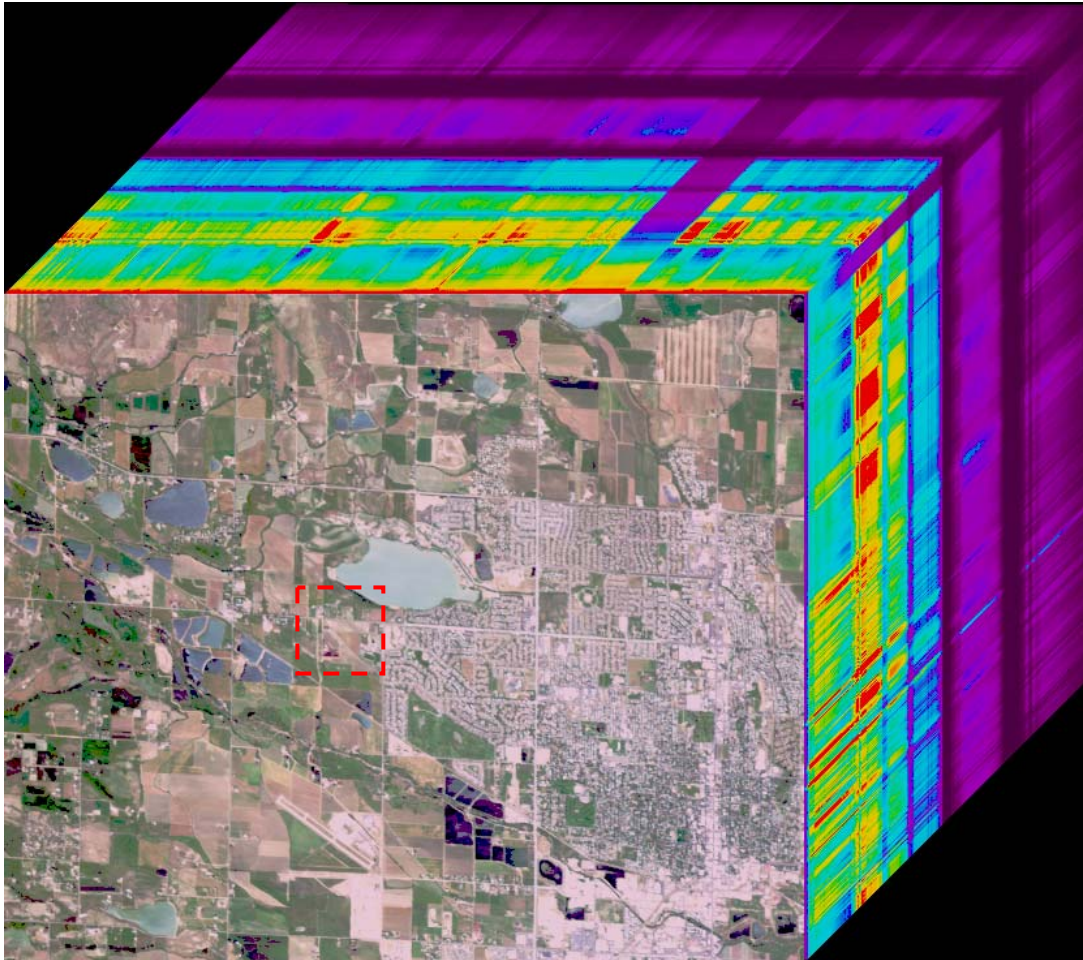
- Atmospheric correction
- Artifacts correction
- Mining of hyper-spectral information



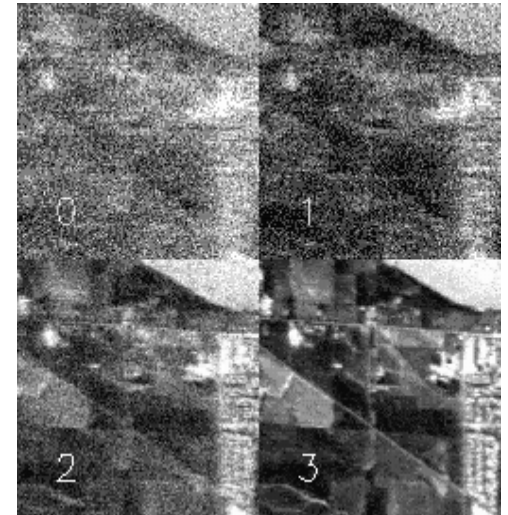
LANL Image Analysis and Understanding Data
From Scientific Experiments Dec. 2-6, 2002



Example: AVIRIS image of Denver*

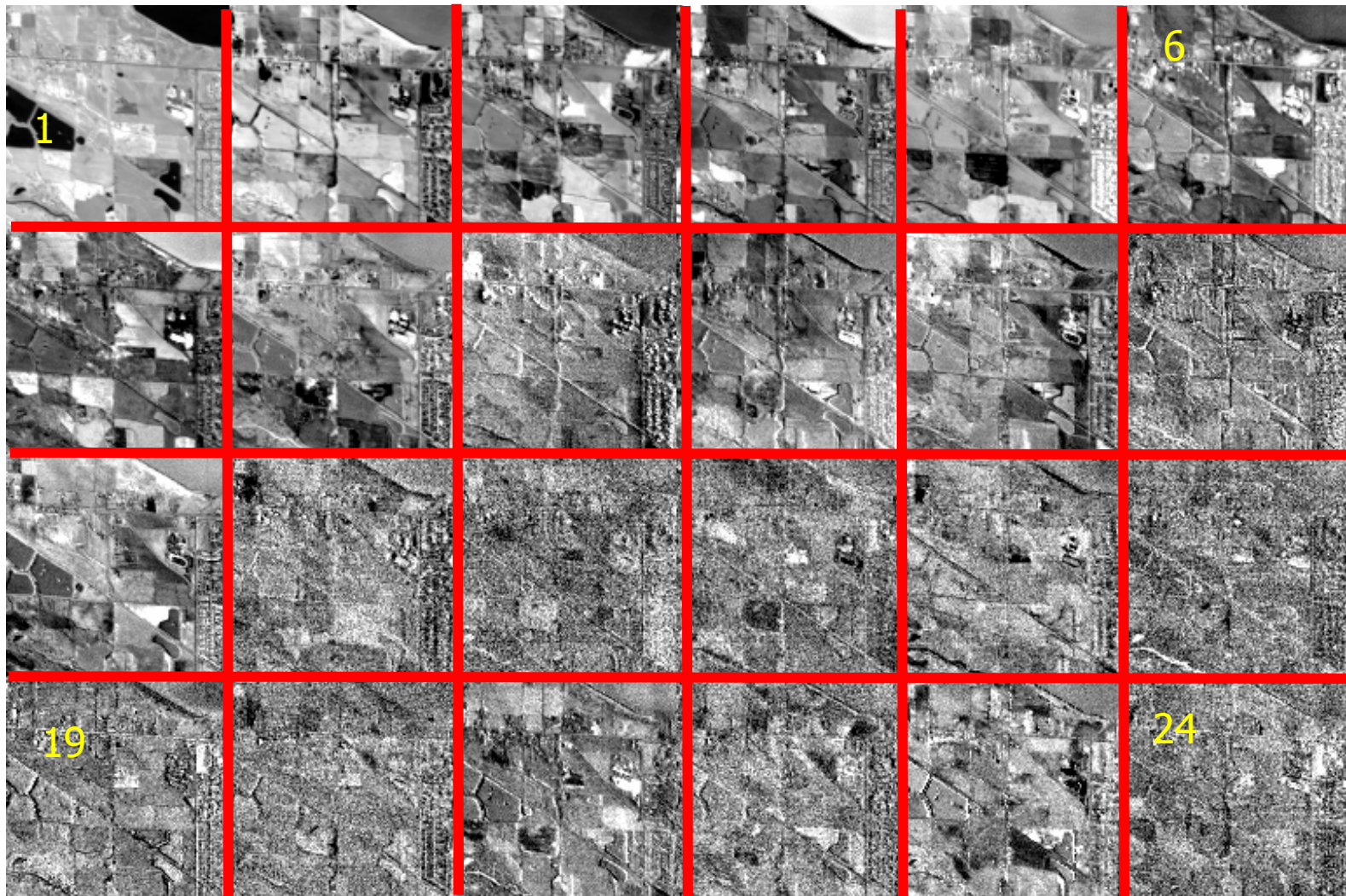


- Sides of cube show spectrum
- Dark lines are atmospheric absorptions
- Movie of 128x128 subset is below with 4 frames shown



* AVIRIS is a NASA airborne sensor with 224 spectral bands

24 Principal components (PC) of 224 channel dataset



Properties of good hyperspectral datasets

- 100's to 1000's of spectral bands
- Continuous spectral coverage with spectral bands spaced at least by the spectral width
- Each pixel has the same spectral band center and width
- Signal-to-noise greater than 100 for bands in atmospheric windows
- Co-registered images (less than 0.1 pixels RMS)
- Calibrated to radiance using NIST calibrated standards (FEL lamps and black bodies)

Processing required for a hyperspectral dataset*

- Calibration: convert digital numbers into radiances
- Atmospheric correction of measured radiance to reflectance for material identification:

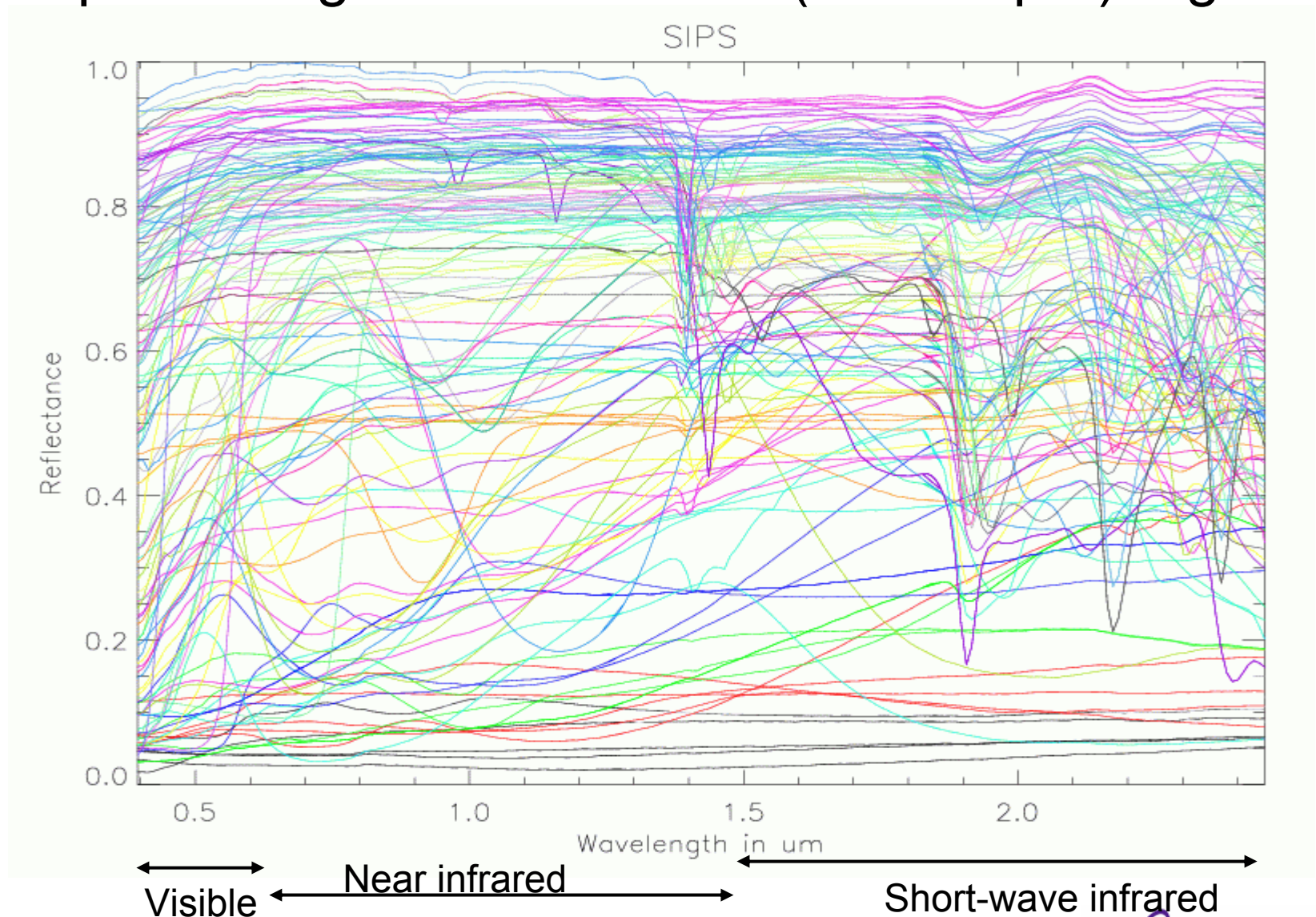
$$L_m = \frac{E_0}{\pi} \cos \theta_s \frac{\tau_s(\theta_s)}{1 - \langle \rho \rangle_s} \left\{ \rho \tau_{direct}(\theta_v) + \langle \rho \rangle \tau_{diff}(\theta_v) \right\} + L_p$$

$$\text{if } \rho = \langle \rho \rangle \text{ then } \rho = \frac{\rho_{ac}}{1 + \rho_{ac}s} \quad \text{where} \quad \rho_{ac} = \pi \frac{L_m - L_p}{E_0 \cos \theta_s \tau_s(\theta_v) \tau(\theta_v)}$$

Where: L_m =measured radiance, ρ =surface reflectance,
 s =spherical albedo of atmosphere
 $\langle \rho \rangle$ =adjacency filtered reflectance, E_0 = solar irradiance,
 τ_s = transmission from sun to surface, $\tau = \tau_{direct} + \tau_{diff}$
 τ_x = direct and diffuse transmission from ground to sensor,
 L_p = path radiance

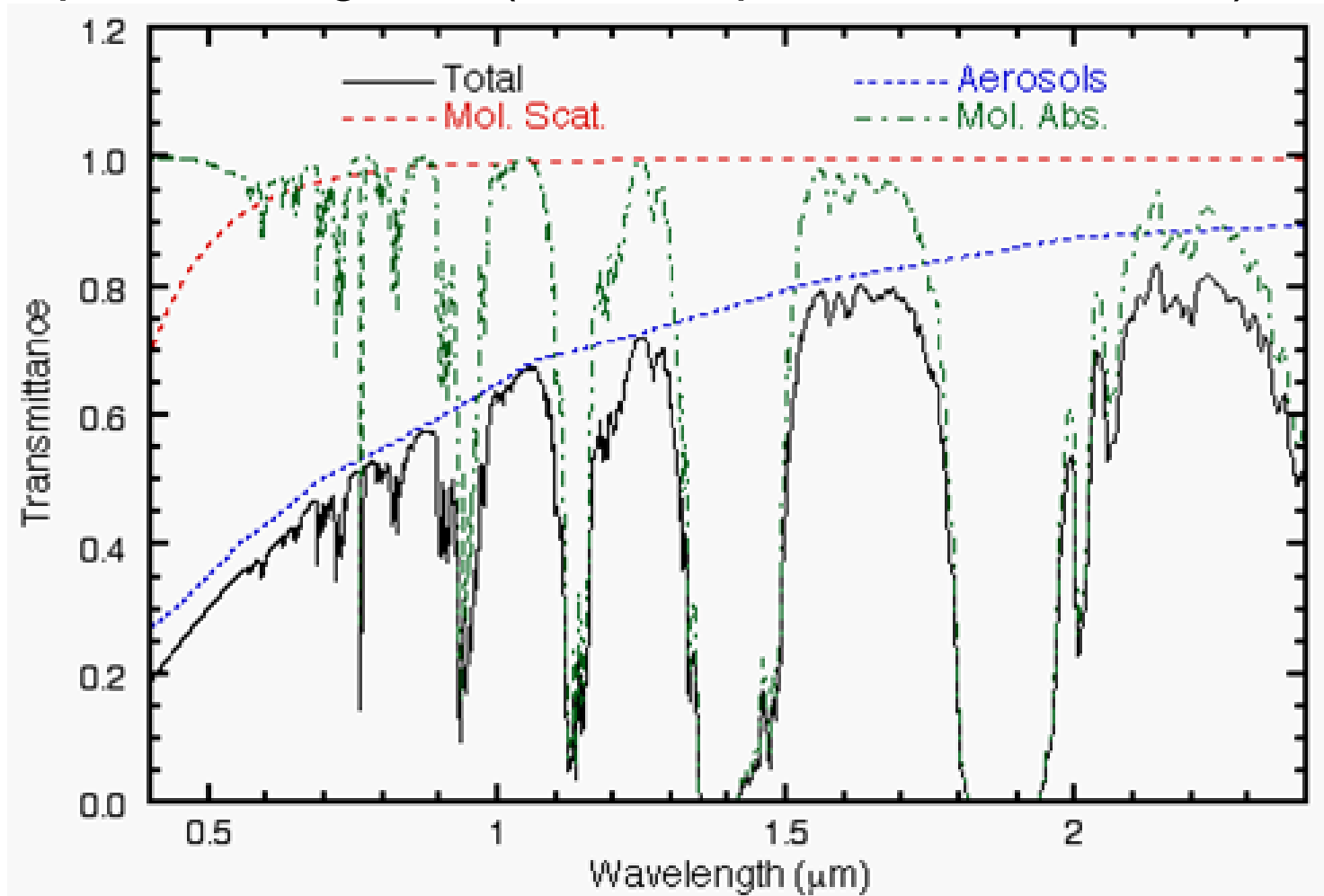
* From FLAASH and 6S codes

Spectral signatures in VNIR (0.4-2.5 μm) region*



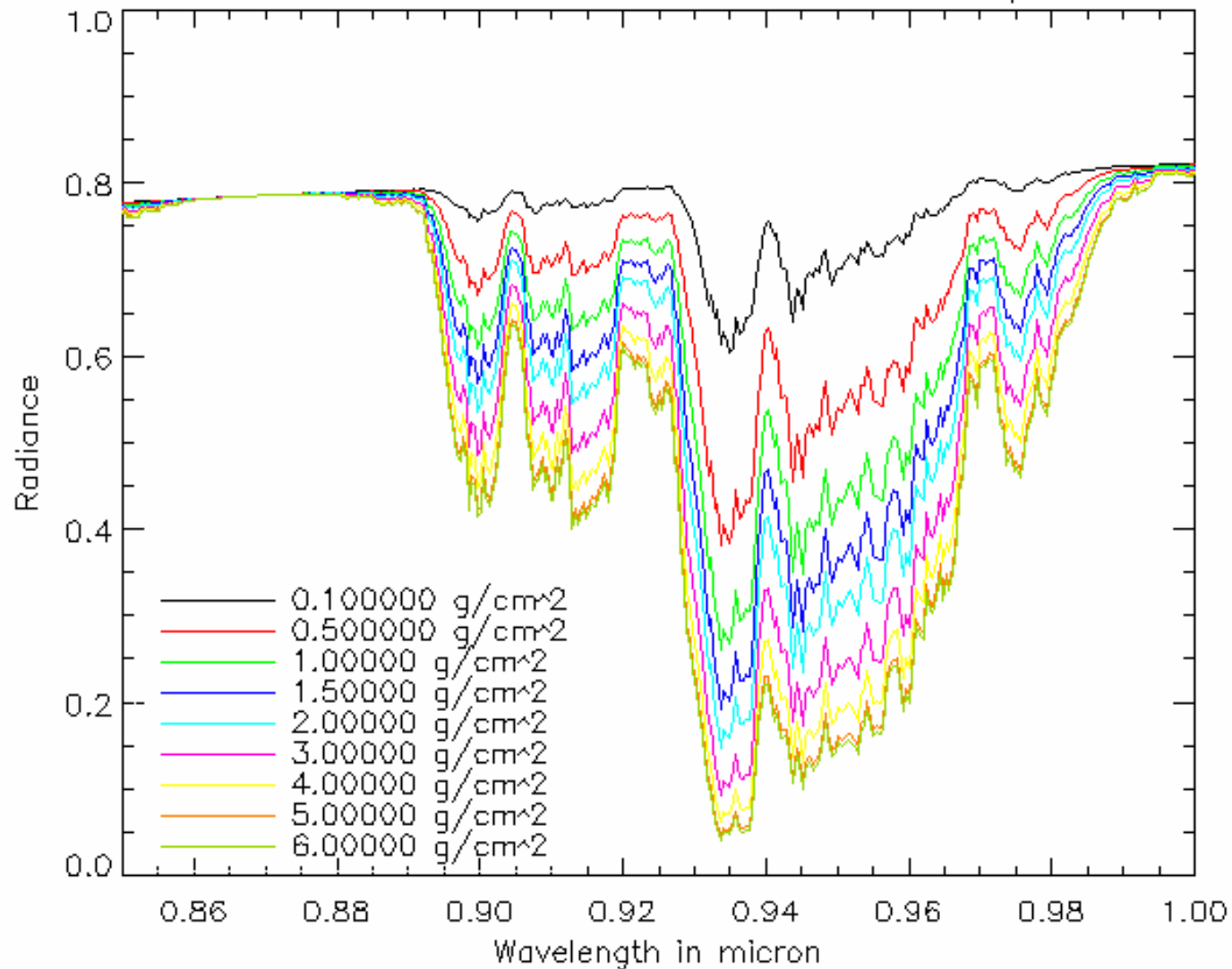
Atmospheric Transmission in the VNIR*

Absorption from gases (water vapor, ozone, CO₂,...)

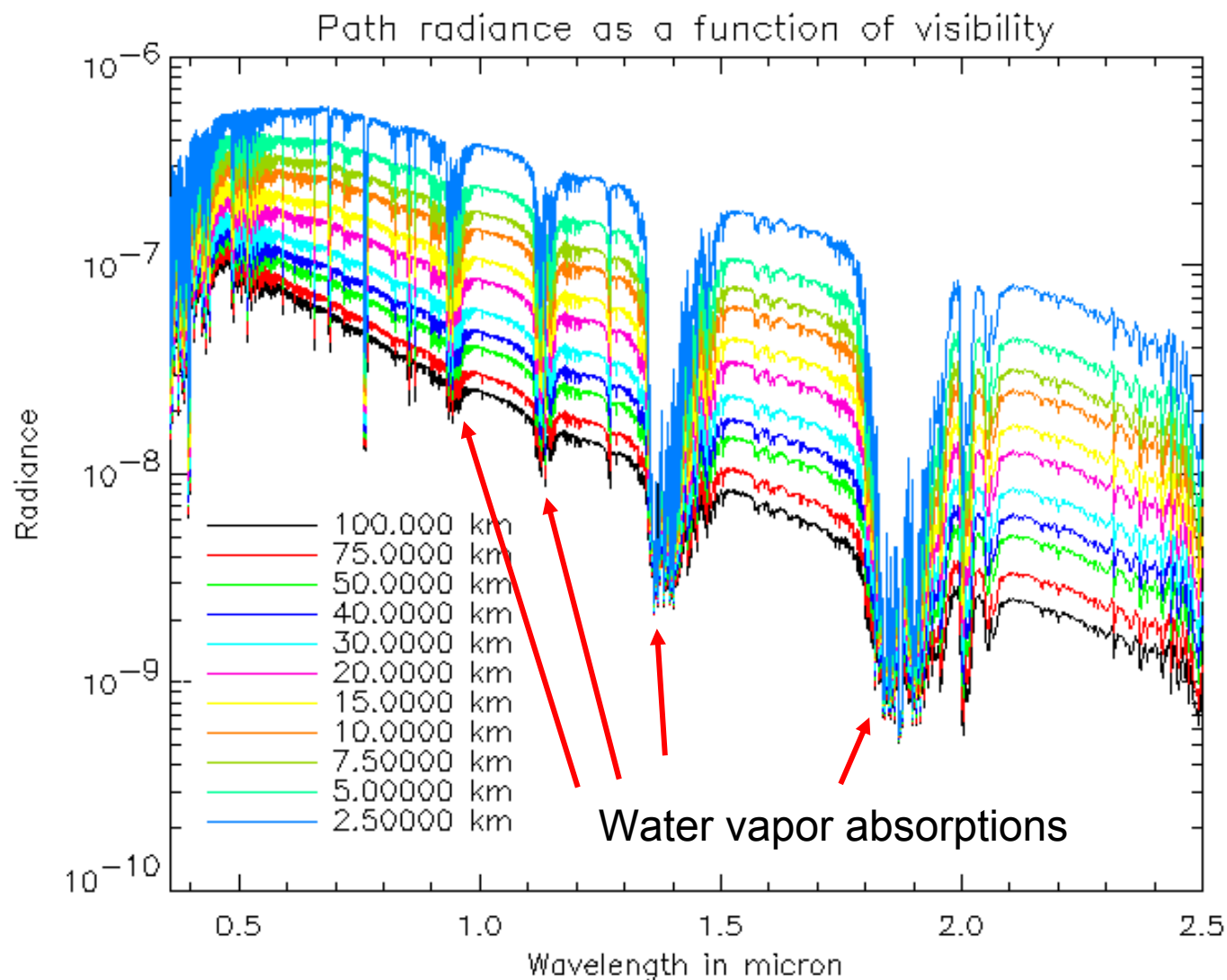


Effect of water vapor on transmission

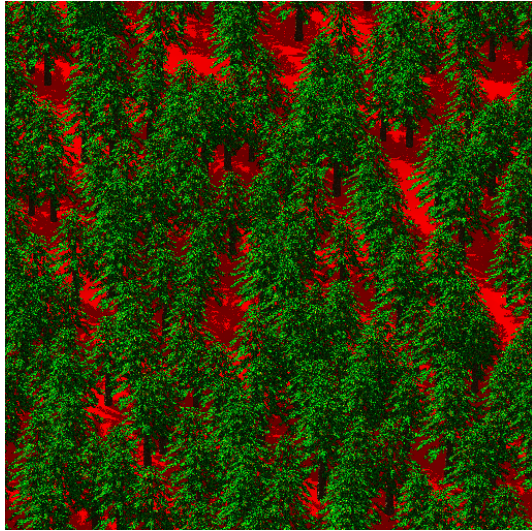
Transmission as a function of water vapor



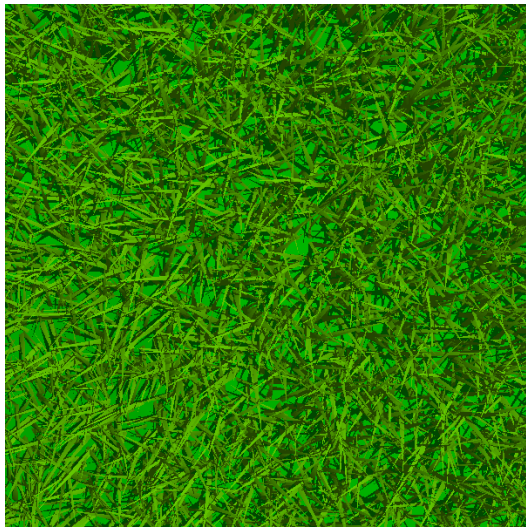
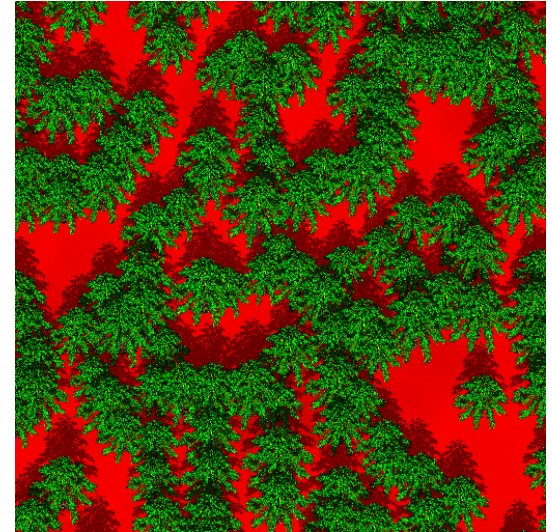
Atmospheric path radiance



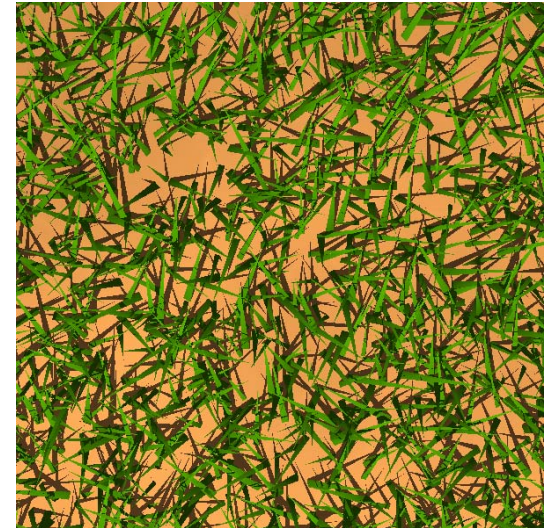
Surfaces appear differently when viewed or illuminated from different directions



Variation with view direction:
Forrest viewed from
Off-nadir (left) and nadir
(right)

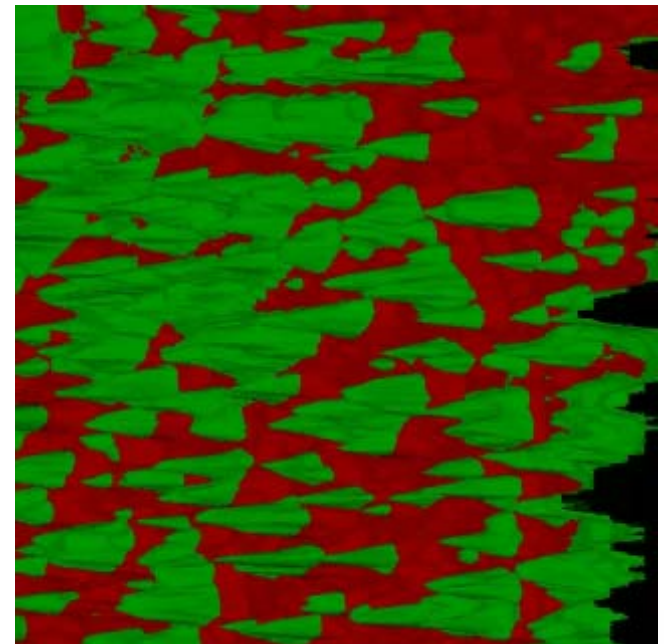
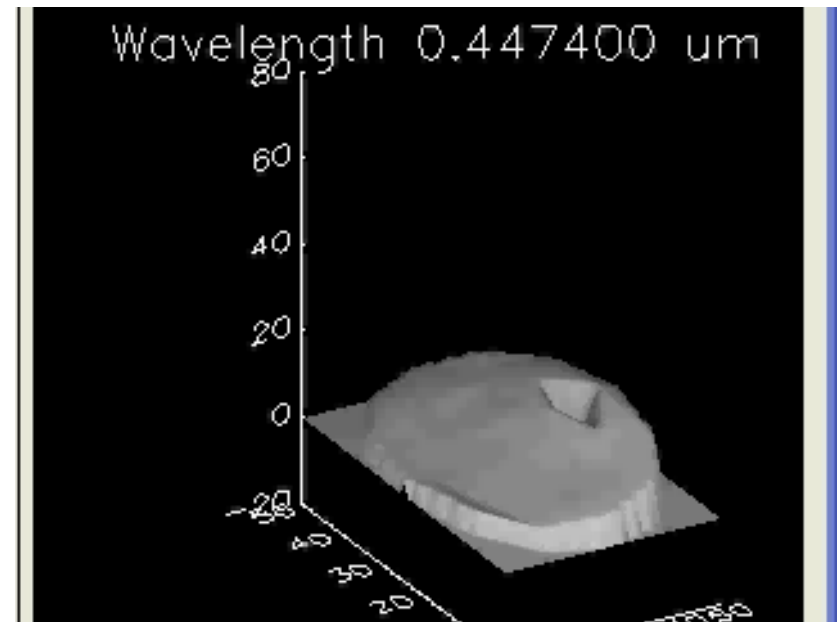


Variation with density:
Dense grass on
The left, thin
Grass on right

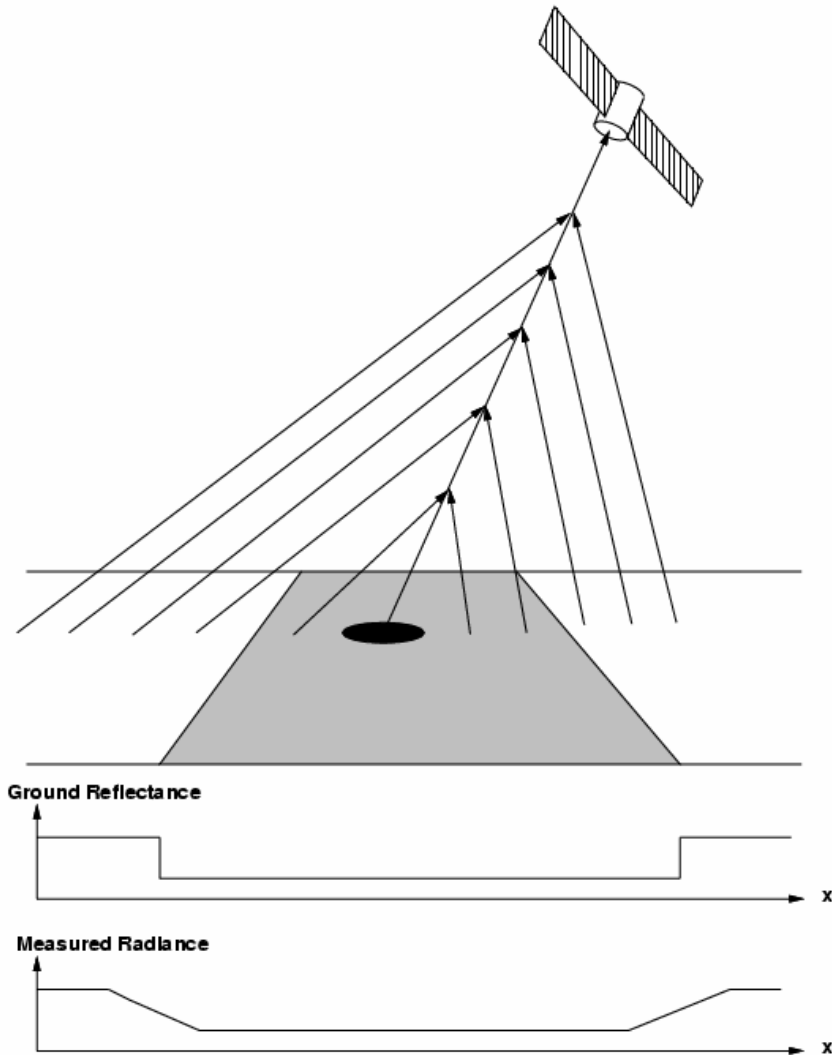


Bi-Directional Reflectance Distribution Function (BRDF) effects

- Surfaces change reflectance as a function of illumination and viewing geometry
- Spectral variations in BRDF shape are due to changes in multiple reflection
- Upper-right shows animation of measured grass BRDF (Sandmeier, U. Zurich) as a function of wavelength
- Lower-right shows animation of LASER range image over Jornada LTER (M. Chopping) as a function of view angle

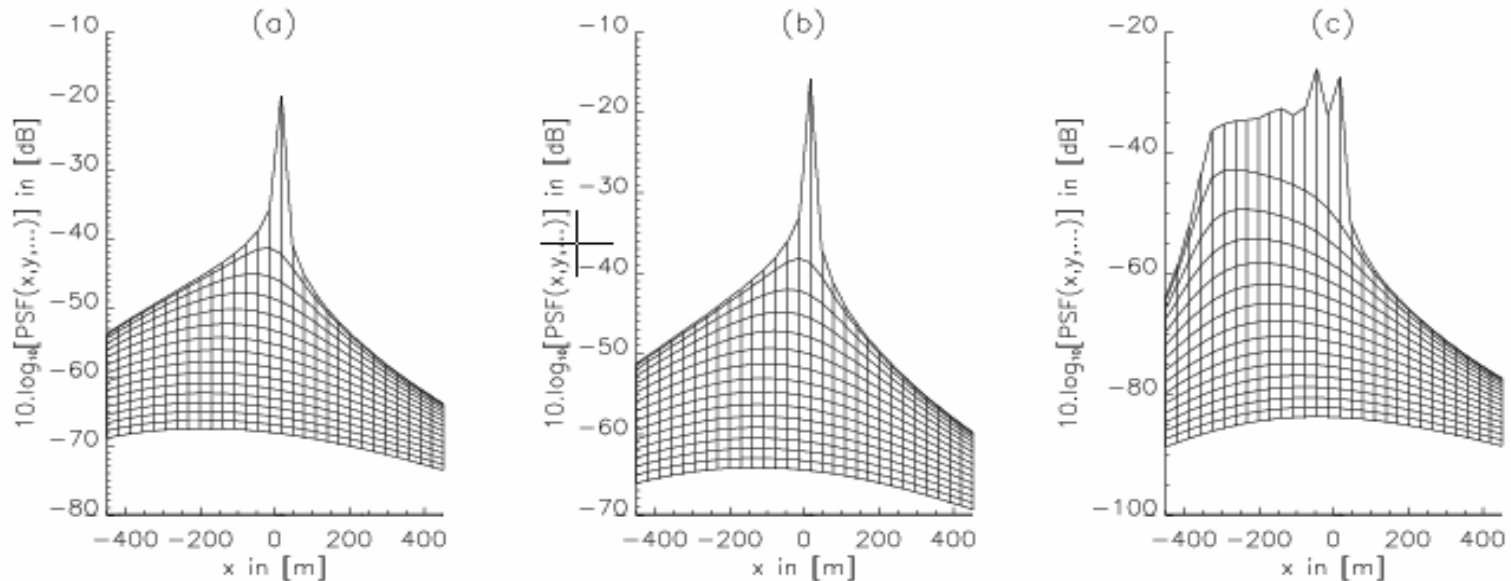


Adjacency blurring due to scattering from nearby surfaces into the line-of-sight



- Blurring amount depends on visibility
- Blurring causes spectral features to “bleed” into dark regions, e.g. vegetation into water surfaces
- Blurring kernel size is in the order of height of boundary layer (1-2 km)
- Blurring point spread function (PSF) is a function of look-angle and surface BRDF
- Blurring reduces contrast

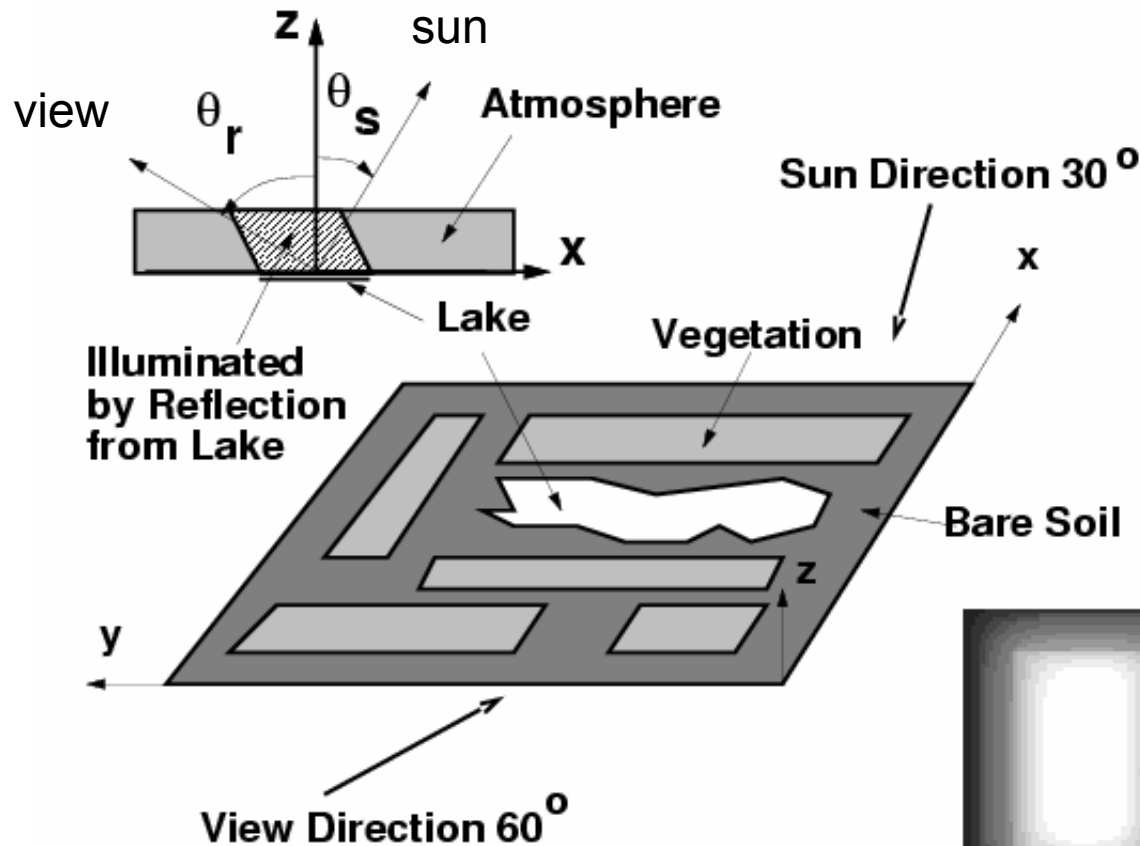
Dependency of adjacency PSF on BRDF*



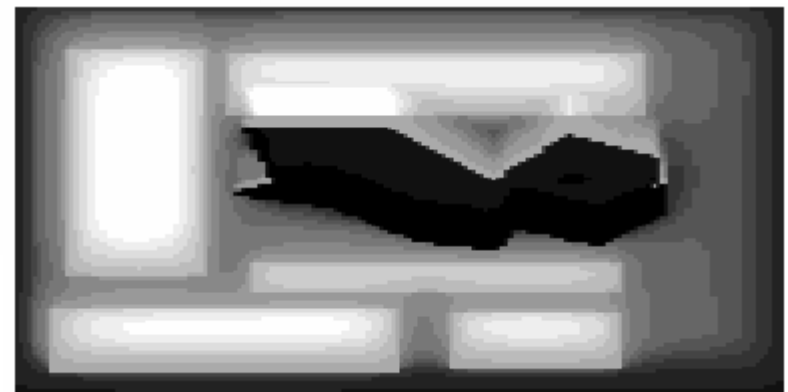
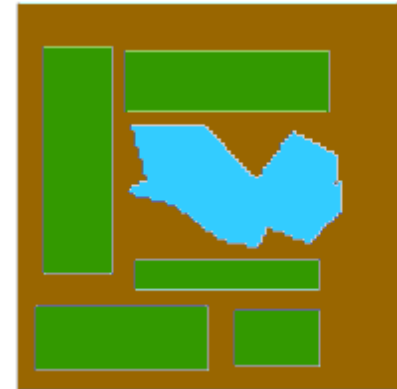
Point spread functions of (a) bare soil, (b) vegetation and (c) water with the z -axis in logarithmic scale and the y -axis points into the paper.

* Borel, 1992

Simulation of a scene with adjacency



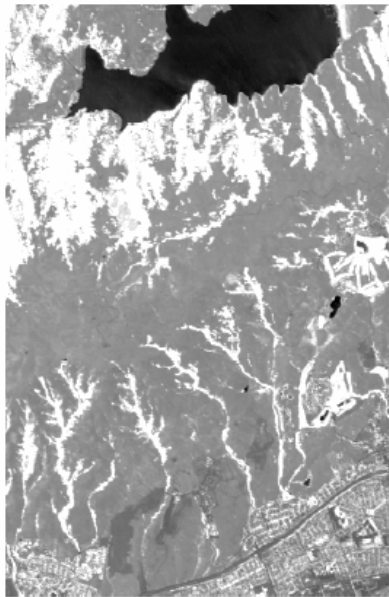
Scene types



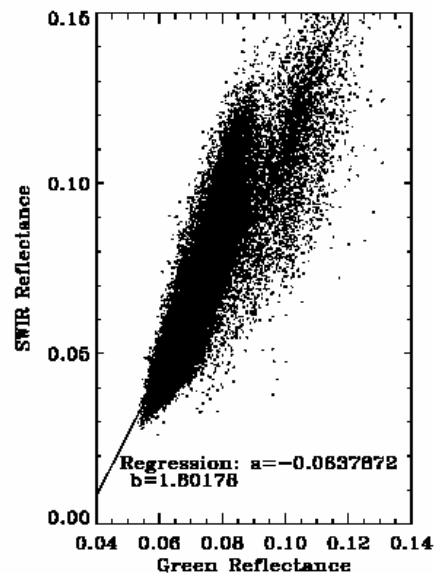
Some approaches for atmospheric correction in the VIS-SWIR

- Estimate visibility by correlation of SWIR (e.g. 2.1 μm) bands to red (0.66 μm) band over vegetation (Kaufman & Tanré)

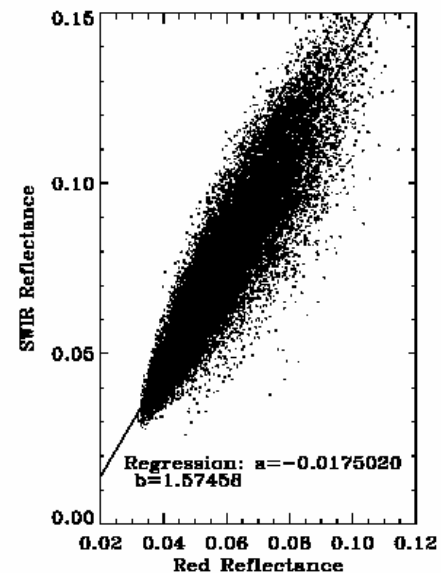
TOA reflectance correlations over dense dark vegetation



a



b

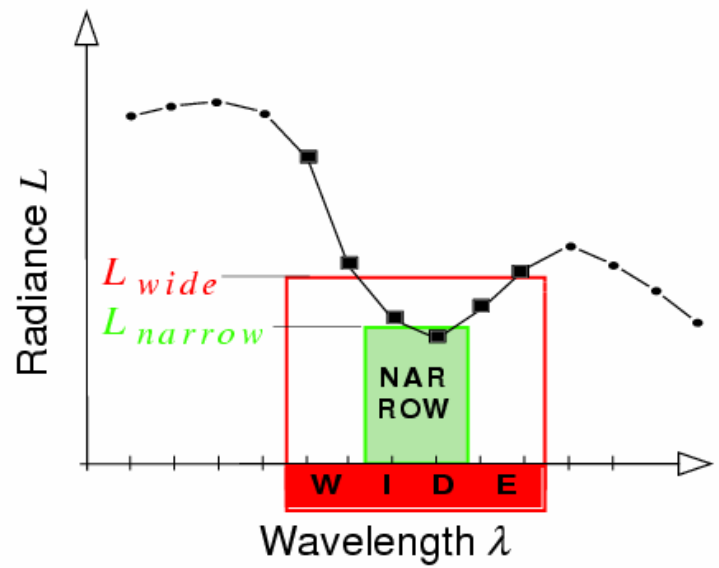


c

(a) NDVI* image (white is where $\text{NDVI} > 0.5$) TOA reflectances in (b) green and (c) red channels correlated to the 2.1 μm SWIR channel for: $(\text{NDVI} > 0.5) \cap (\rho_{2.1 \mu\text{m}} < 0.15)$

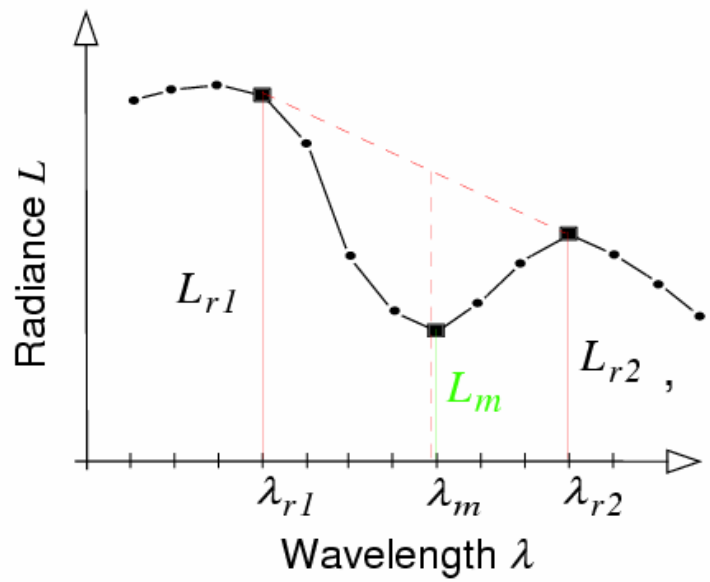
- Estimate water vapor using band ratios near 0.94 μm band*

Narrow/Wide



$$R_{N/W} = \frac{L_{narrow}}{L_{wide}}$$

Continuum Interpolated Band Ratio



$$R_{CIBR} = \frac{L_m}{\omega_{r1} \cdot L_{r1} + \omega_{r2} \cdot L_{r2}}$$

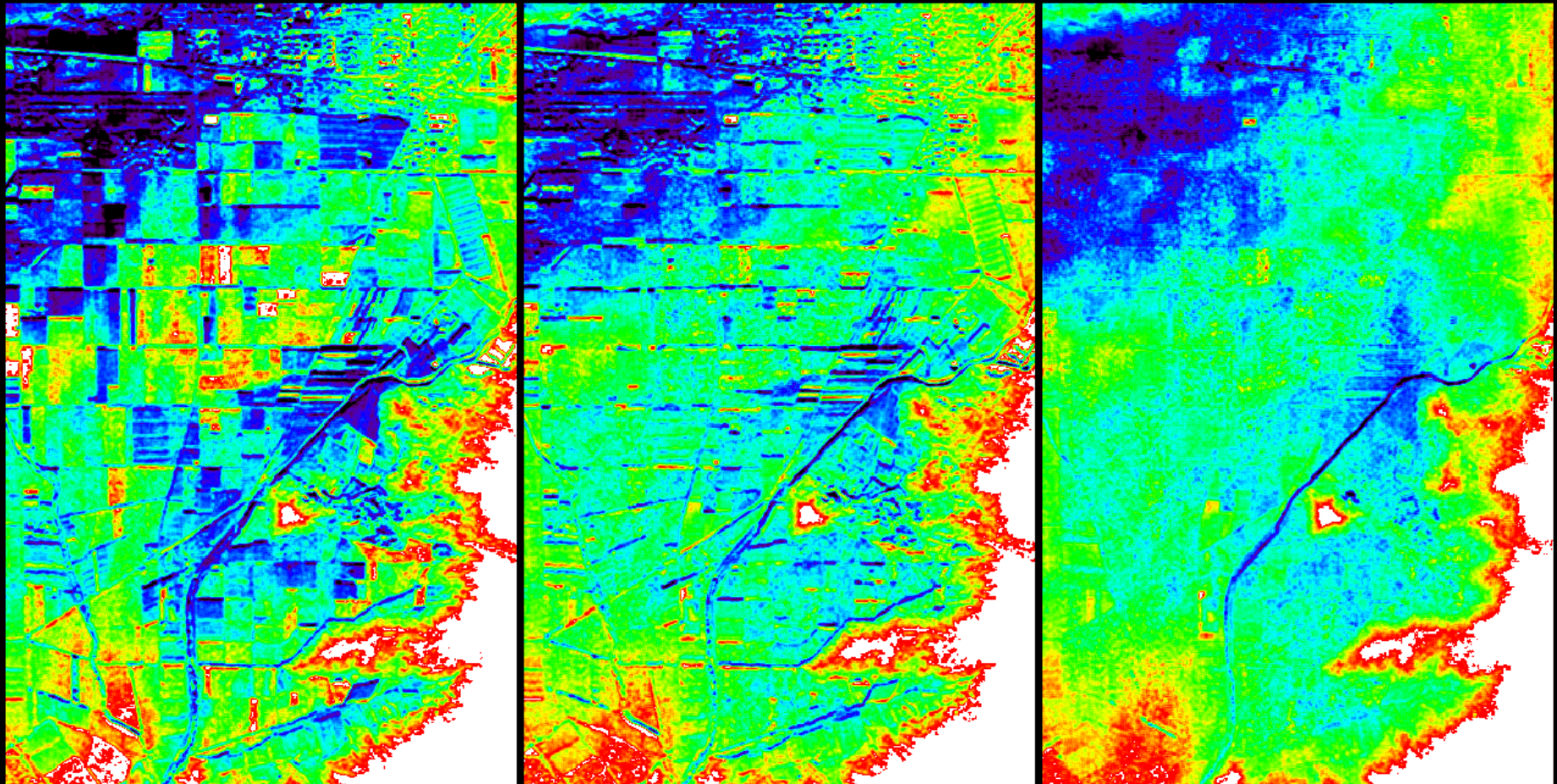
$$\omega_{r1} = \frac{\lambda_{r2} - \lambda_m}{\lambda_{r2} - \lambda_{r1}}$$

$$\omega_{r2} = \frac{\lambda_{r1} - \lambda_m}{\lambda_{r2} - \lambda_{r1}}$$

Water vapor retrieved with aerosol correction (APDA)

Atmospheric Pre-Corrected Water Vapor Retrieval from AVIRIS'95 Data

Scene Camarillo, 5-26-95, run 8, scene 3; enhanced over the plain between Camarillo and Point Mugu, mountain area appears white



LIRR processing, uncorrected

APDA processing

APDA processing, shift corrected

Total Columnar Water Vapor (range):

20 kg/m²

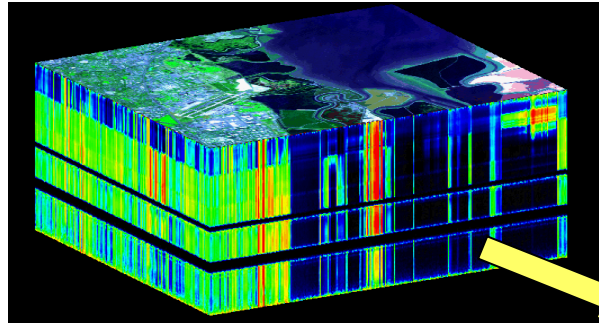


17 kg/m²



D.Schlaepfer, RSL/LANL, 1-96

FLAASH*: Fast Line-of-sight Atmospheric Analysis of Spectral Hypercubes



Hyperspectral
image cube



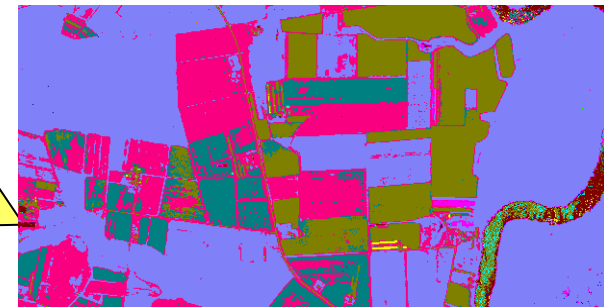
Uncorrected
radiance image

FLAASH atmospheric correction



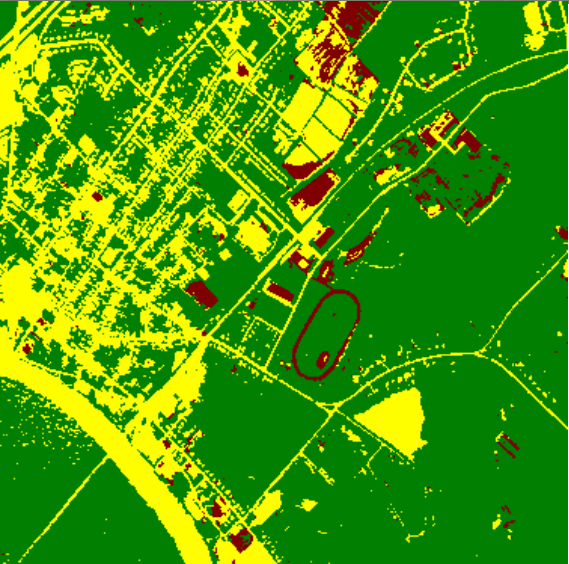
Atmospherically corrected
reflectance image

Classification map

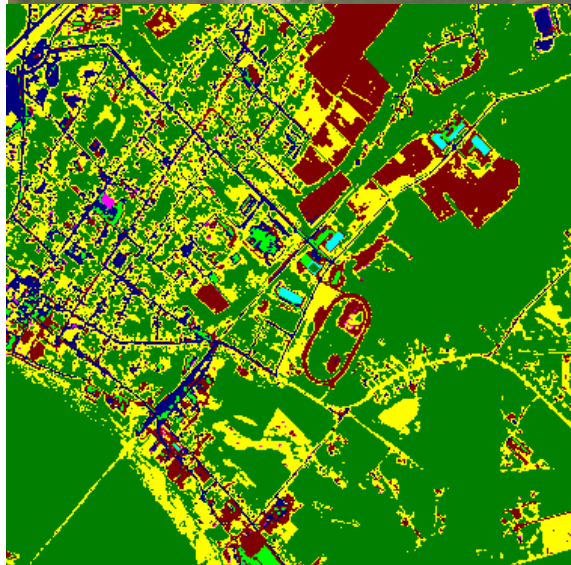


FLAASH adjacency correction increases number of classes*

Radiance



Reflectance (no adj.)



Reflectance (with adj.)



Measured radiance in the thermal infrared

- Measured radiance in the thermal infrared:

$$L_{\text{measured}}(\lambda) = L_{\text{ground}}(\lambda) + L_{\text{gas}}(\lambda) + L_{\text{path}}(\lambda)$$

$$L_{\text{ground}}(\lambda) = [\varepsilon(\lambda)B(\lambda, T_{\text{ground}}) + (1 - \varepsilon(\lambda))L_{\text{down}}(\lambda)]\tau_{\text{atmo}}(\lambda)\tau_{\text{gas}}(\lambda)$$

$$L_{\text{gas}}(\lambda) = [1 - \tau_{\text{gas}}(\lambda)]B(\lambda, T_{\text{gas}})$$

$$L_{\text{path}}(\lambda) = [1 - \tau_{\text{atmo}}(\lambda)]B(\lambda, T_{\text{atmo}})$$

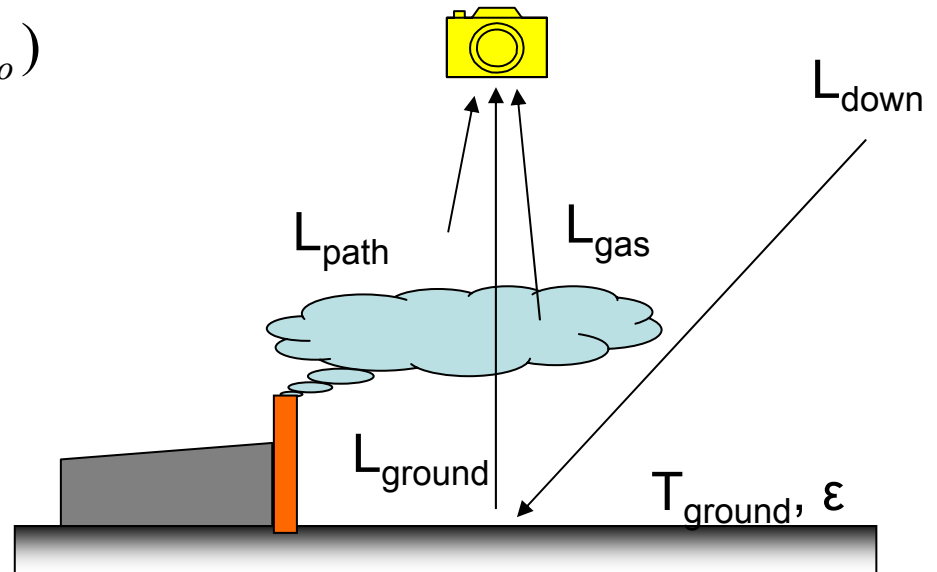
where :

$\varepsilon(\lambda)$ = spectral emissivity

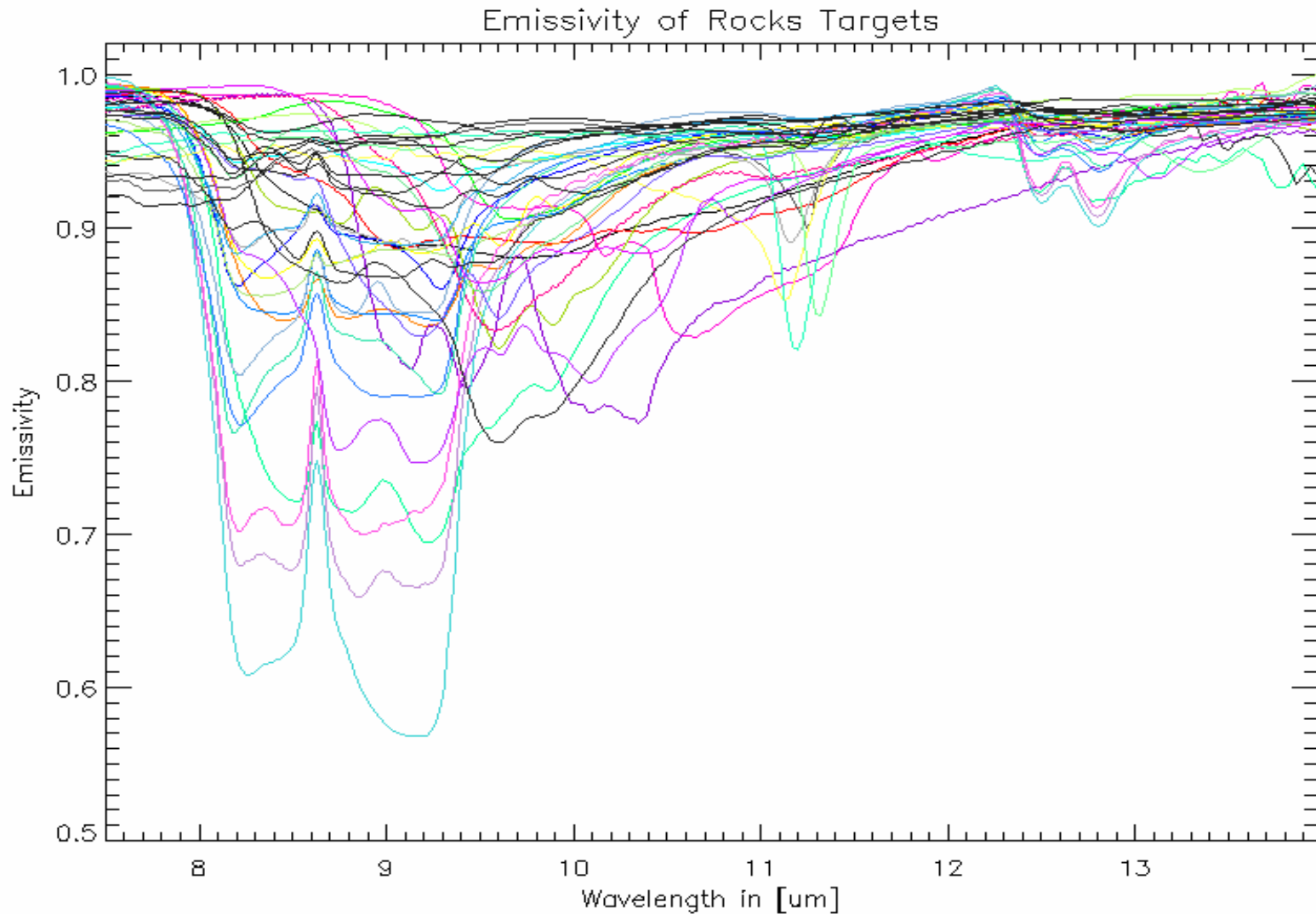
$\tau_x(\lambda)$ = spectral transmission

$B(\lambda, T)$ = Planck function

T_x = Temperature

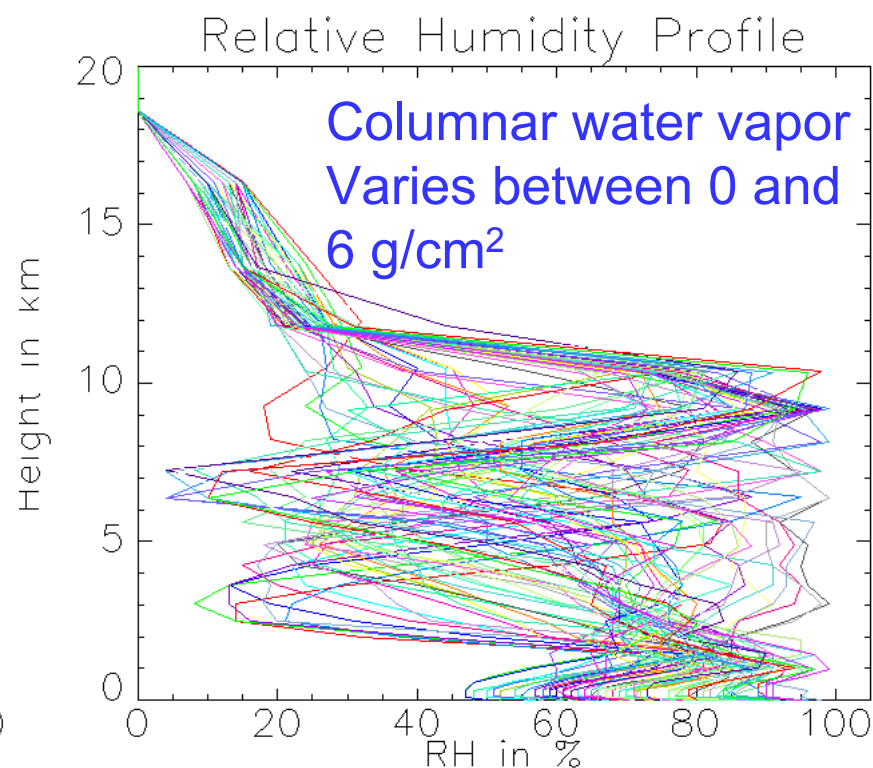
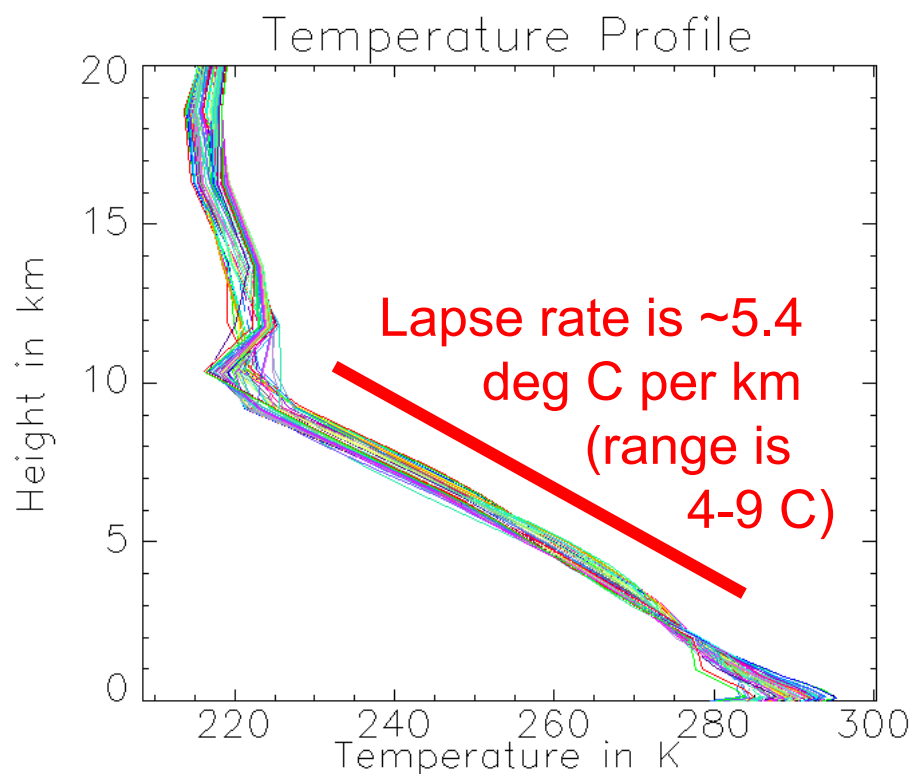
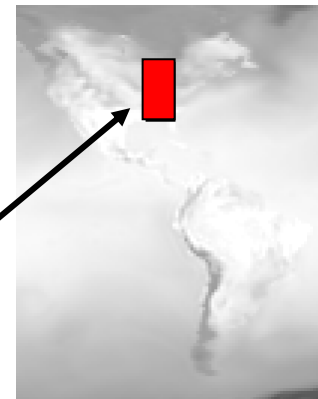


Spectral signatures in the thermal IR (7.5-14 μm)*



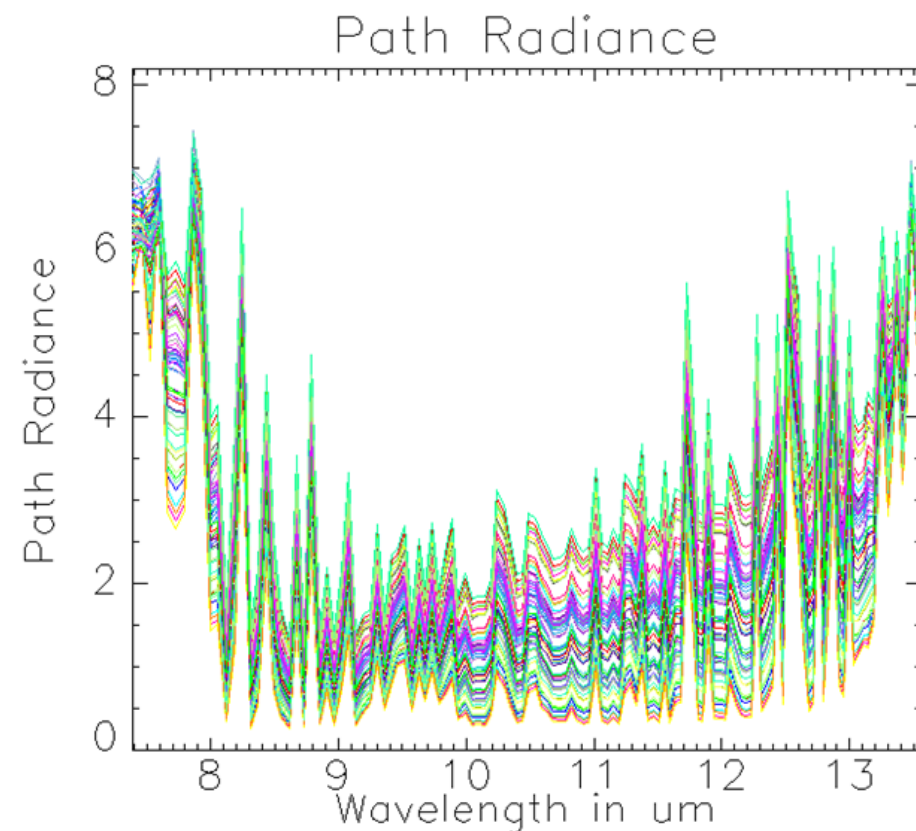
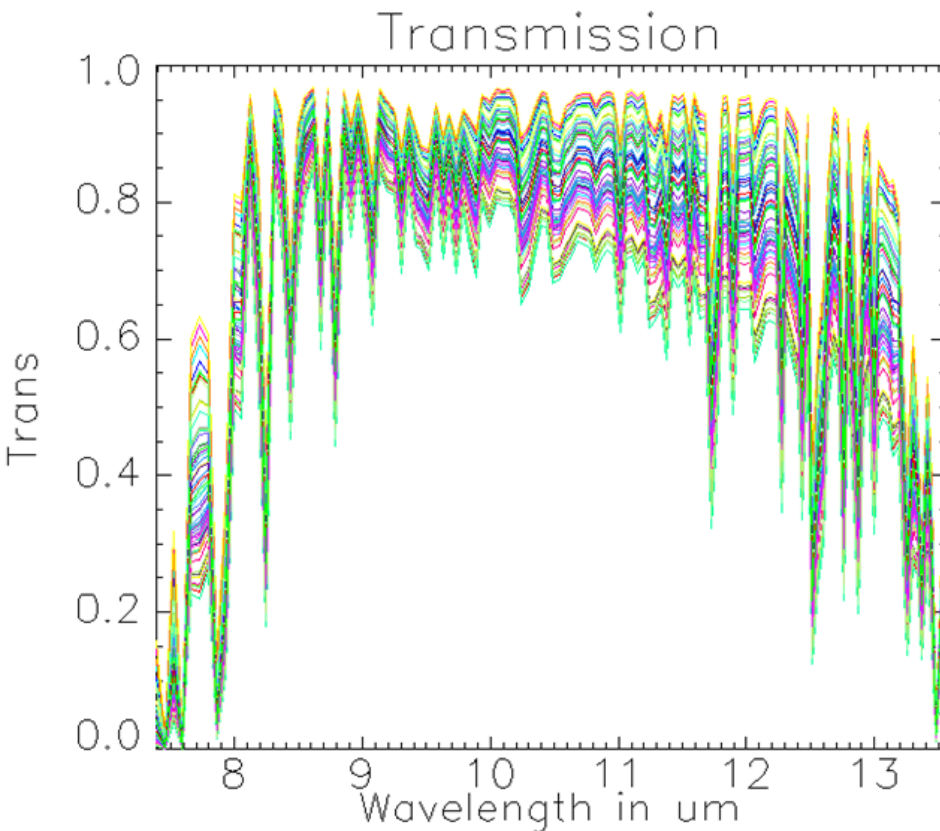
Atmospheric variability

Cloud free pixels in a 10 deg by 20 deg Region of Global Data Assimilation System (GDAS)* for 18h GMT for May 28, 2001



Variability in transmission and path radiance

Notice: The atmospheric features have sharp absorption features compared to emissivities!

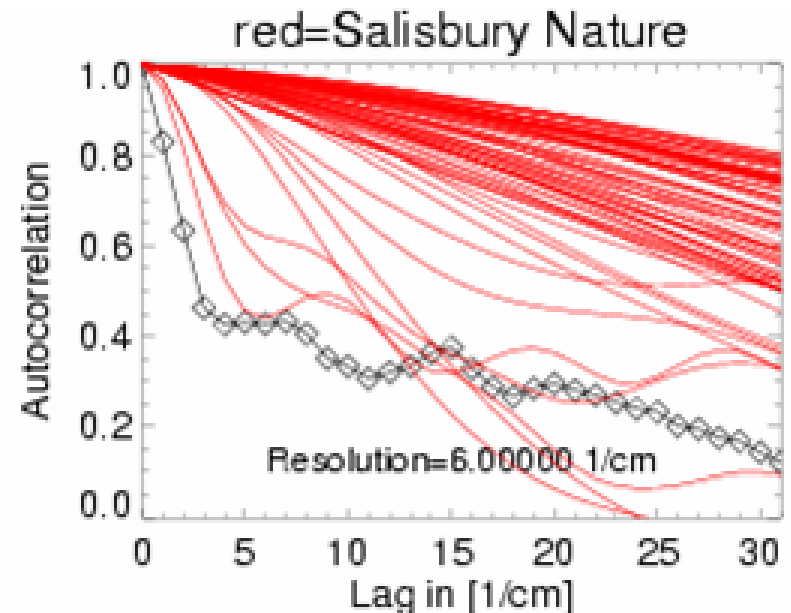
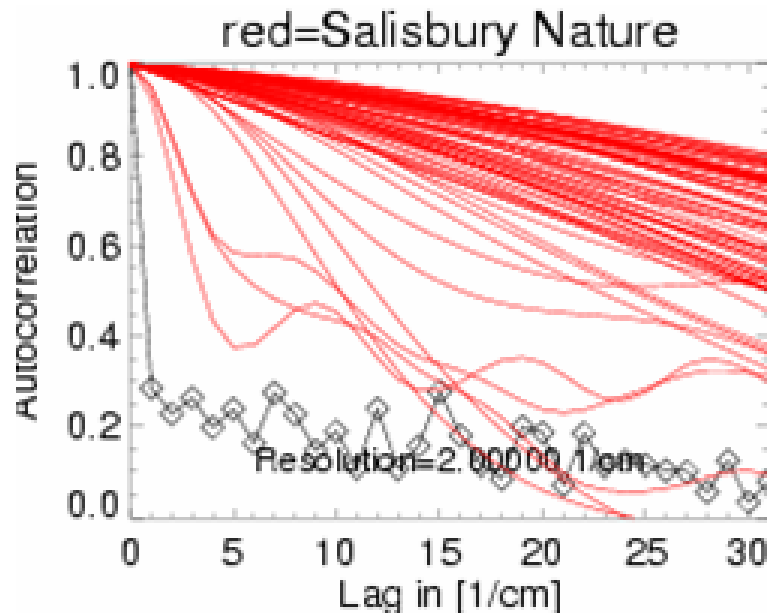


Retrieval of T_{ground} and $\epsilon(\lambda)$

Underdetermined problem: Given the at sensor radiance retrieve temperature T and emissivity ϵ in N bands for a unknown atmosphere (temperature profile, relative humidity profile and total ozone amount) \rightarrow more than N unknowns!

Solution: Take advantage of the fact that emissivity changes slower with wavelength than atmospheric transmission and path radiance

Atmosphere decorrelates faster than emissivity of materials:



Automatic Retrieval of Temperature and Emissivity using Spectral Smoothness (ARTEMISS*) algorithm

Algorithm:

1. Use the “In-Scene Atmospheric Correction” (ISAC) method to get an estimate of transmission
2. Find best fitting atmosphere in look-up-table (LUT)
3. Compute the blackbody temperature T_{bb} in an atmospheric window from an atmospherically corrected surface radiance L_{cor}
4. Compute emissivity: $Emissivity = L_{cor} / B(\lambda, T_{bb})$
5. Try out different temperature offsets ΔT and re-compute emissivity iteratively.
6. Iterate 3-5 until emissivity has fewest atmospheric features or is smoothest.

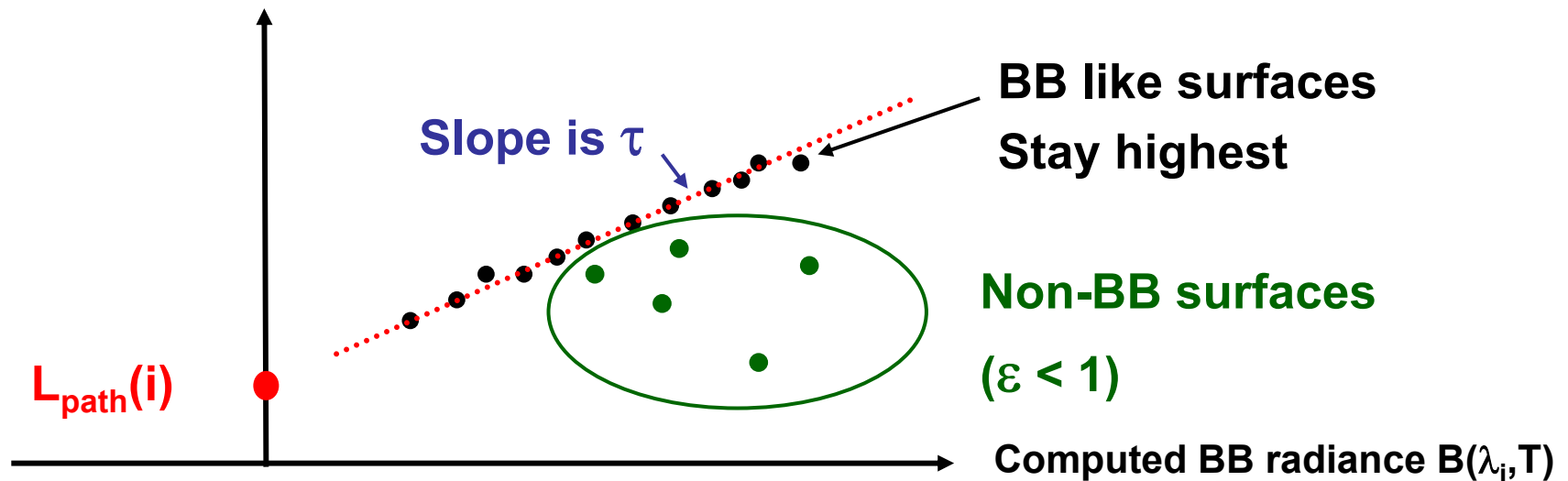
In-Scene Atmospheric Correction* (ISAC)

Assumptions:

- Atmosphere uniform over scene
- Surfaces present which have near blackbody ($\epsilon \approx 1$) characteristics (e.g. water, vegetation,...):

$$L_m(\lambda_i) = B(\lambda_i, T)\tau_i + L_{\text{path}}(i)$$

Measured radiance in band m: $L_m(\lambda_i)$



Smooth emissivity retrieval method*

Steps:

1. Compute the initial ($n = 0$) blackbody temperature $T_{bb,n}$ in an atmospheric window from an atmospherically corrected radiance $L_{cor,0}$:

$$T_{bb,n} = B^{-1}(\lambda_{window}, L_{cor,n})$$

with

$$L_{cor,n} = \frac{L_{total} - L_{path\uparrow}(CW, T_{atmo}) - L_{path\downarrow}\varepsilon(n)}{\varepsilon(n)\tau_{atmo}(CW)},$$

where CW stands for column water, T_{atmo} is the effective atmospheric temperature and $\varepsilon(0) = 0.95$.

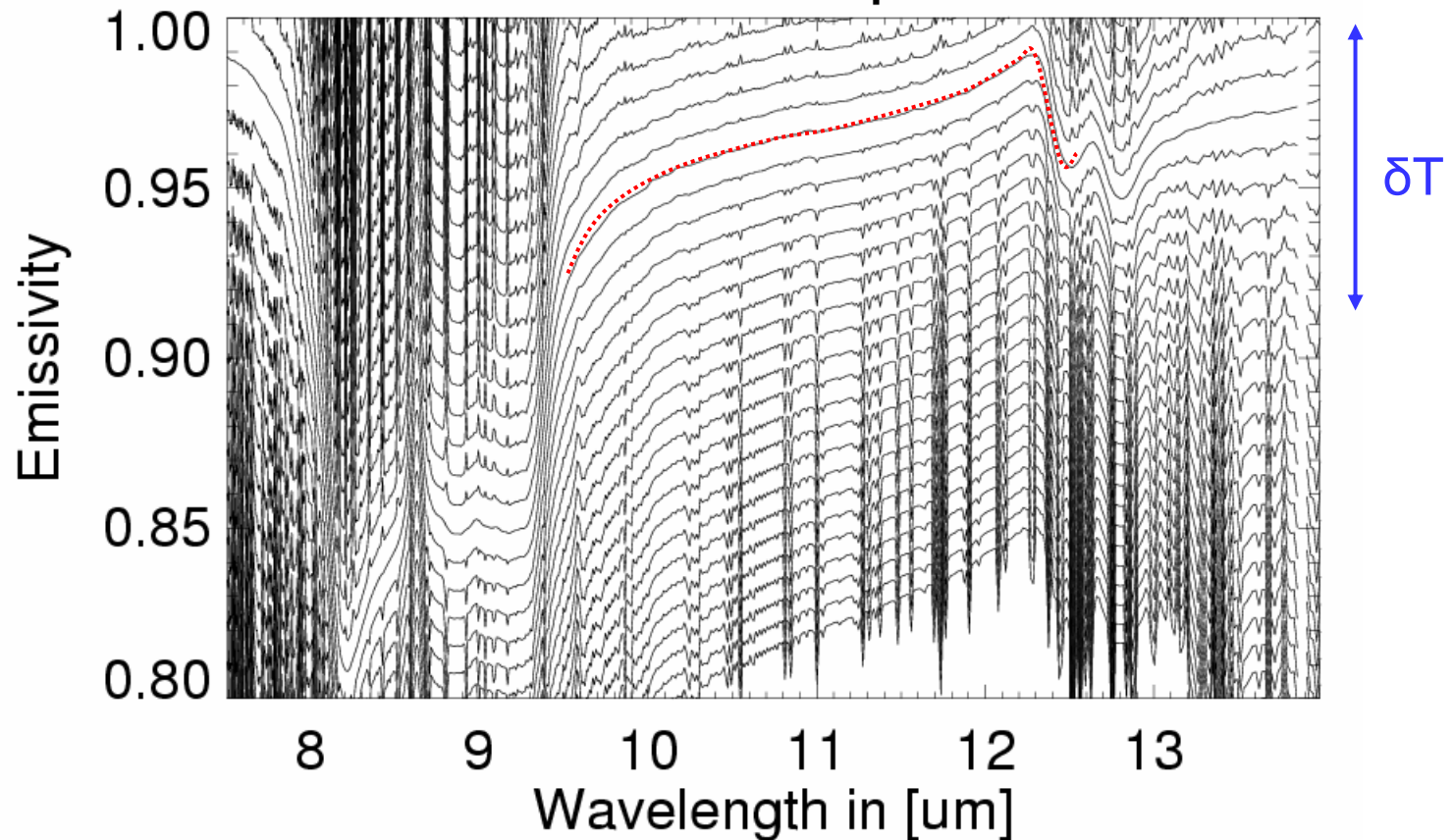
2. Compute spectral emissivity: $\varepsilon(n) = L_{cor,n}/B(\lambda, T_{bb,n})$, $n = 1, 2, \dots$
3. Vary the surface temperatures $T_{bb,n} = T_{bb,0} + i\Delta T$, $i = 1, 2, \dots$, change the columnar water amounts and the effective atmospheric temperatures and recompute $\varepsilon(n)$ iteratively using steps 1-3.
4. Stop iteration when emissivity is smoothest, i.e. when

$$\sigma(\varepsilon(n)) = STDEV \left[\varepsilon_i(n) - \frac{1}{K} \sum_{j=i-K/2}^{i+K/2-1} \varepsilon_j(n) \right]_{i=K/2+1, \dots, M-K/2} = Min,$$

where the spectrum consists of M channels.

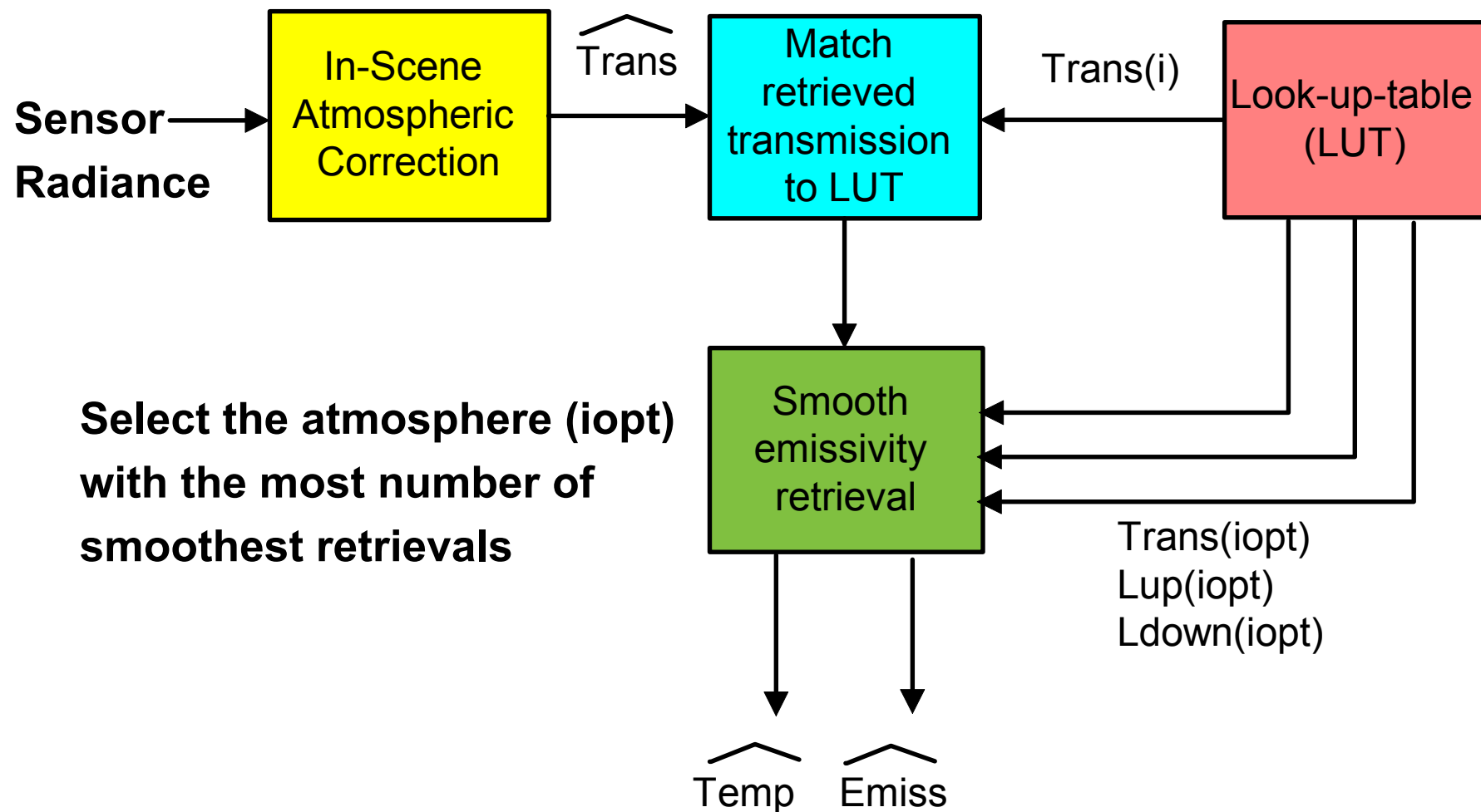
Iterative temperature retrieval to find **smoothest** emissivity

Iterations to find Temperature Offset

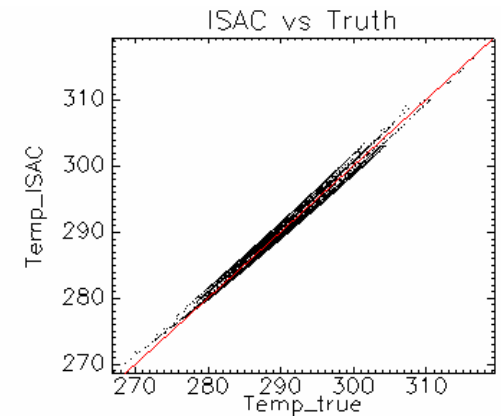
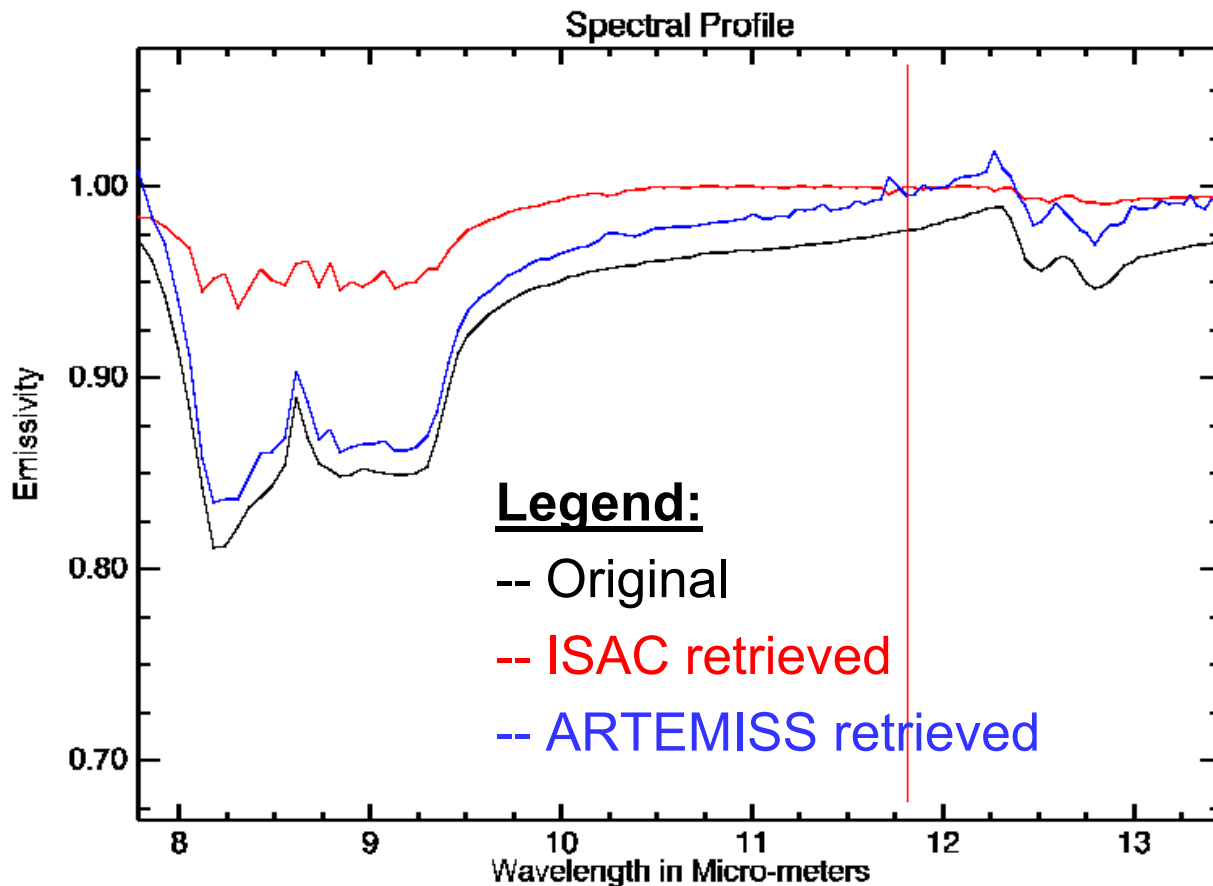


Retrieved emissivity as a function of temperature offset δT

ARTEMISS flow diagram

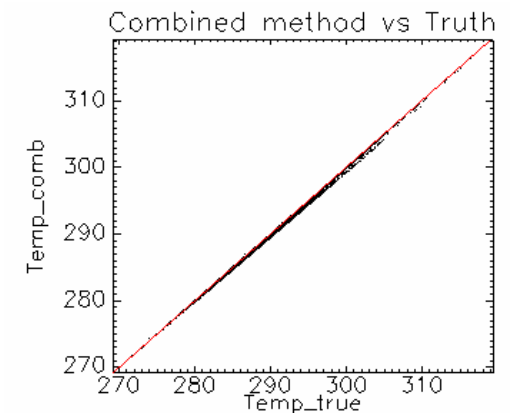


Emissivity and temperature errors using ISAC and ARTEMISS



$$\sigma_{\text{ISAC}} = 0.81 \text{ C}$$

$$\sigma_{\text{ARTEMISS}} = 0.15 \text{ C}$$



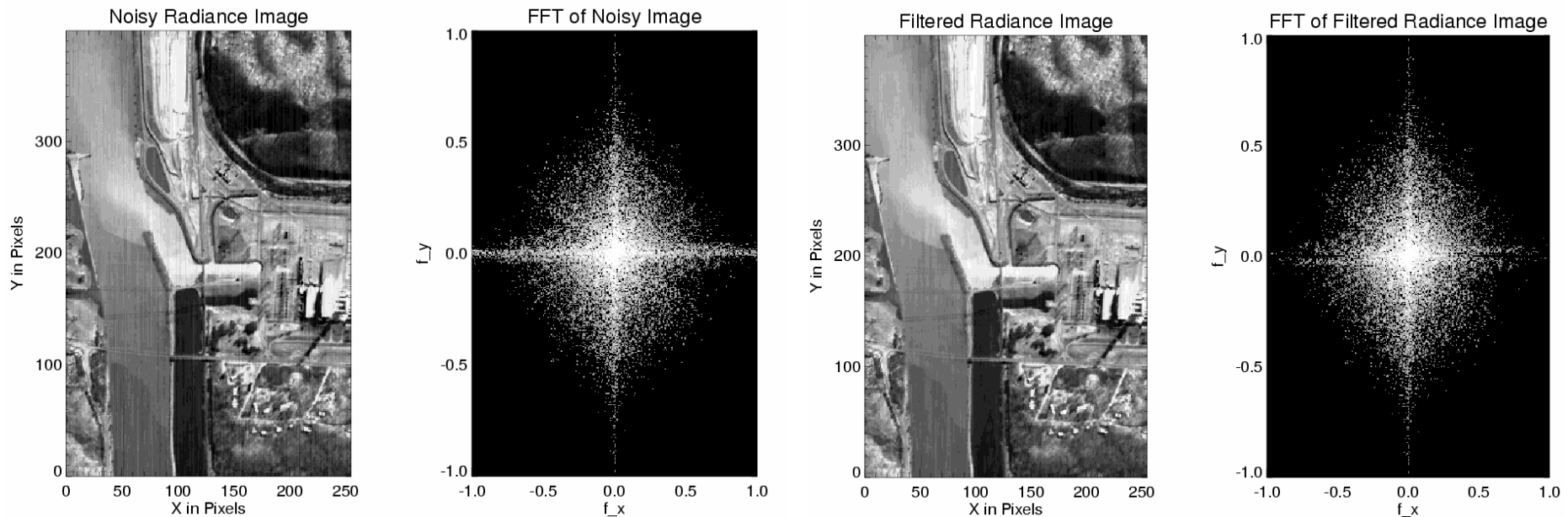
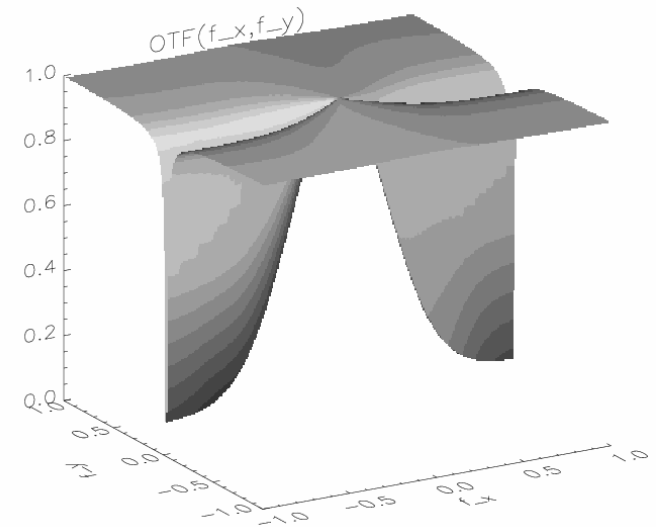
Sensor artifacts

Examples of artifacts:

- Striping (e.g. Landsat has 16 detectors with slightly different linear responses)
 - Correlated noise (e.g. AVIRIS has 400 Hz power supply ripples in data, 1/f noise, read-out noise)
 - Amplifier artifacts (e.g. some amplifiers in AVIRIS have a slew-rate differences – see PC and APDA images earlier)
 - Non-linear detector response (e.g. MCT detectors)
 - Channel to channel misalignment (e.g. due to pointing jitter)
 - Spectral shifts and smile (band-centers shift as a function of pixel position)
 - Ghost images, dead pixels, channeling, sample position errors for FTS, optical path differences in imaging FTS, spectral and spatial aliasing, stray light, ...
- Artifacts can have big effect on data analysis and algorithms and need to be corrected if possible

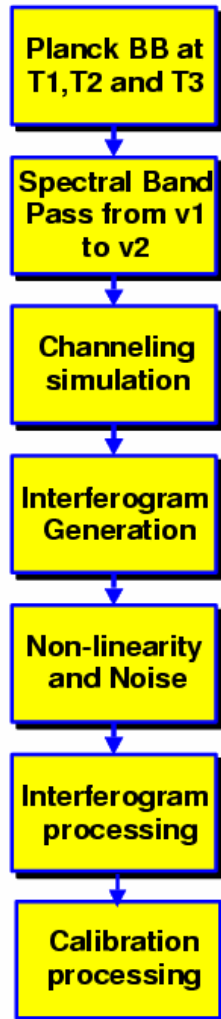
Example of de-stripping data*

- Problem: Some thermal detectors exhibit correlated ($1/f$) noise which introduces striping in the along-track direction
- Solution: Whitening filter (on right) to eliminate noise away from origin of 2-D FFT



Artifacts simulation for imaging Fourier Transform Spectrometers (FTS)*

Parameters for simulations:

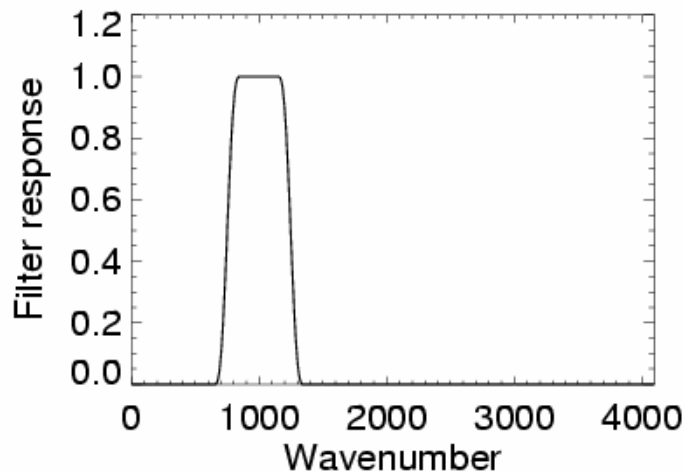


- 3 calibration sources at temperatures $T_0 = 20C$, $T_1 = 30C$ and $T_2 = 40C$, signal to noise ratio $SNR = 1000$, number of samples $N_f = 4096$ frames, and a responsivity between 750 and 1250 cm^{-1} (in-band).
 - Phase dispersion model: $\phi(\nu) = 500(\frac{\nu}{\nu_{max}})[1 + 0.3(\frac{\nu}{\nu_{max}})^2]$
 - Channeling amplitude: $amplitude(\nu) = (1. + 0.2 \cos(\omega_0 \nu))$
 - Nonlinear model: $DN(nonlin) = DN(lin)^d$ where $d = 0.33$
 - Relative position sampling errors in sample units:
 - Periodic: $\Delta Z(z) = a_0 \sin(2\pi \frac{z}{\delta z})$
 - Random: $\Delta Z(z) = b_0 N(m = 0, \sigma = 1) \otimes LP - filter(cut - off = 0.1\nu_{max})$
- where a_0 and b_0 are selected so that the standard deviation $STDEV(\Delta X)$ is 0.02 and 0.001 of a sampling distance.

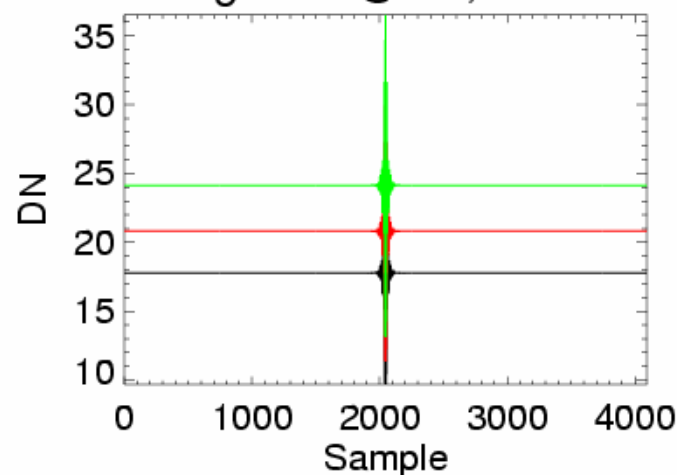
* Borel et al, CALCON'99 talk

Linear FTS simulation

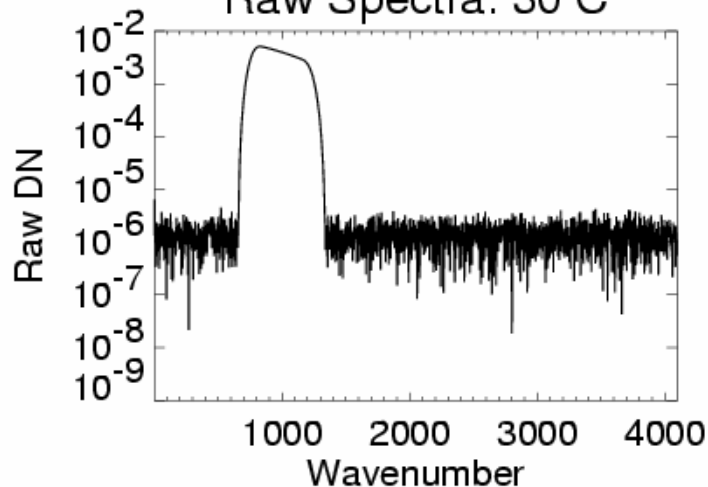
Filter function



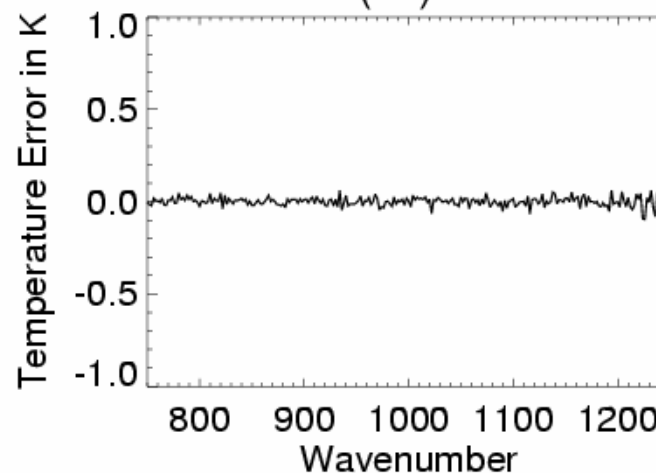
Interferograms @ 20,30 and 40 C



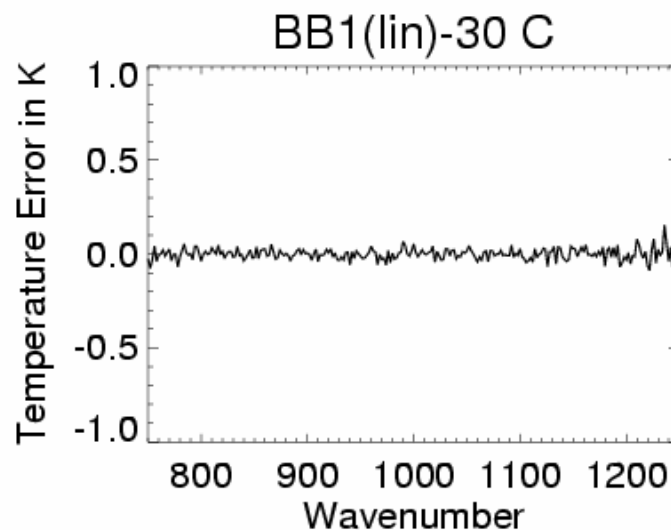
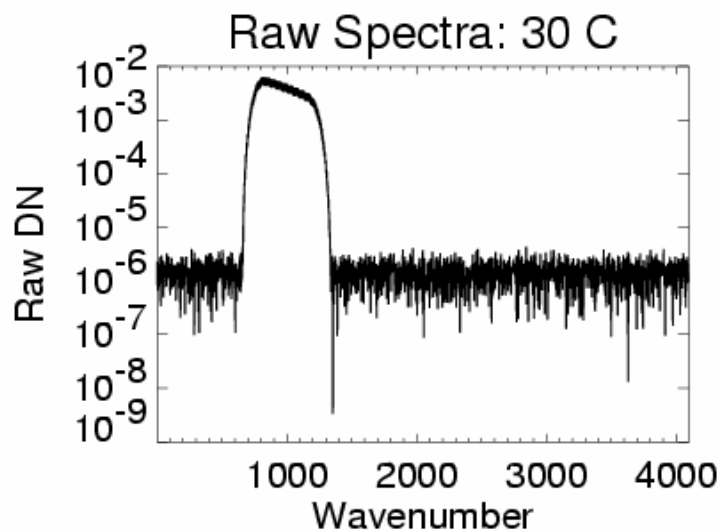
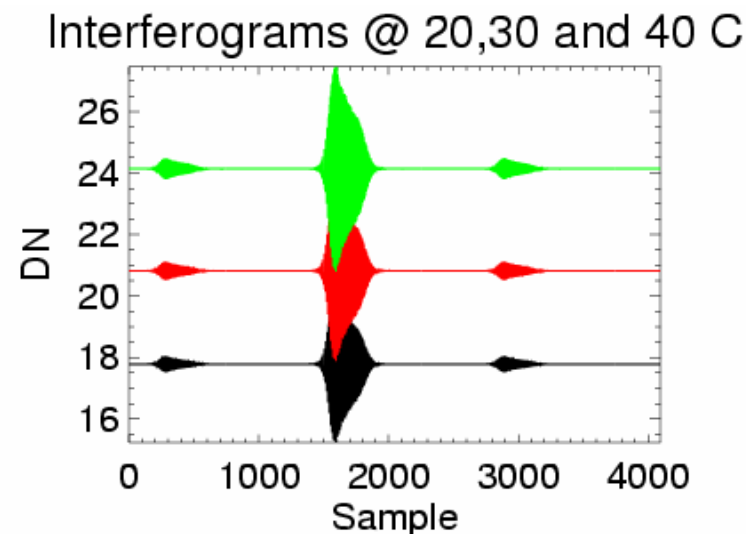
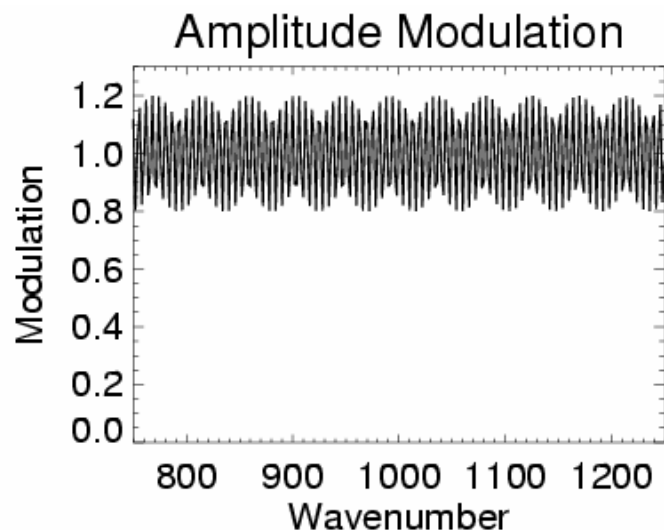
Raw Spectra: 30 C



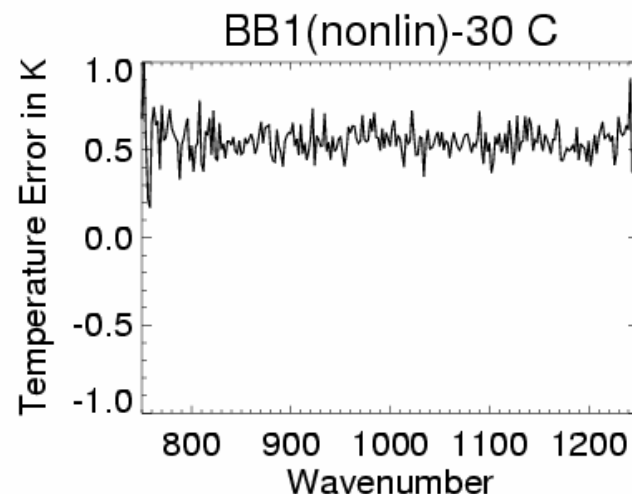
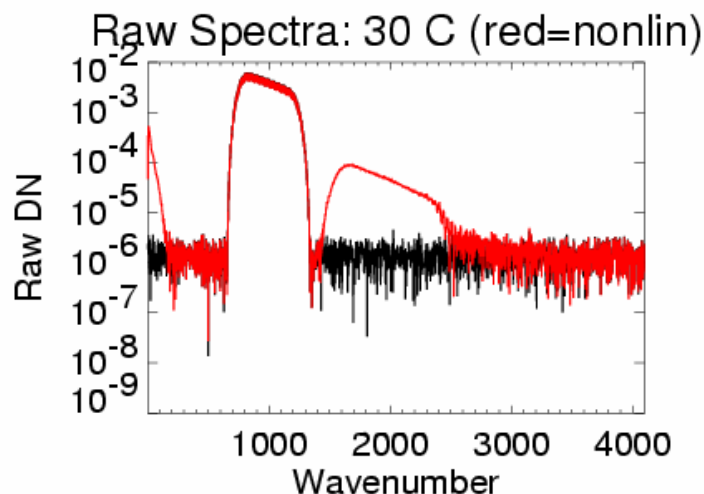
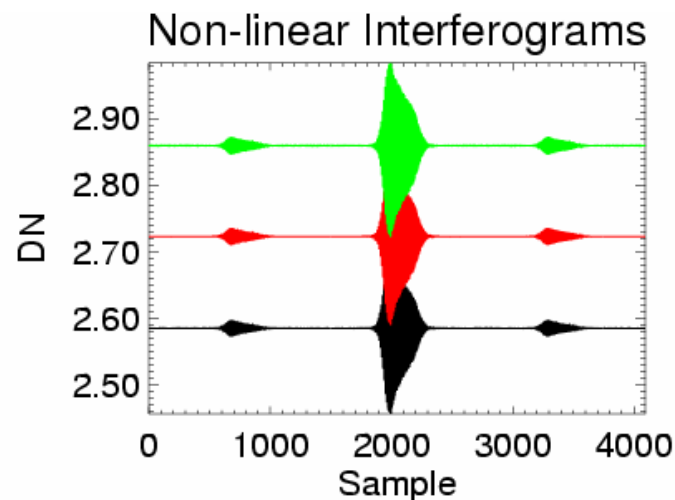
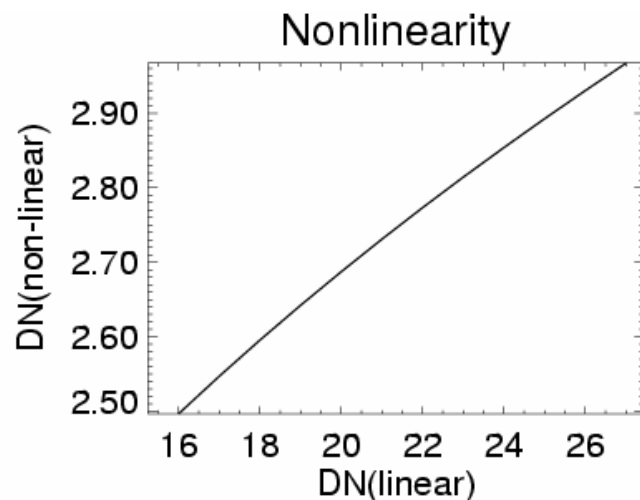
BB1(lin)-30 C



Linear + dispersion + channeling FTS

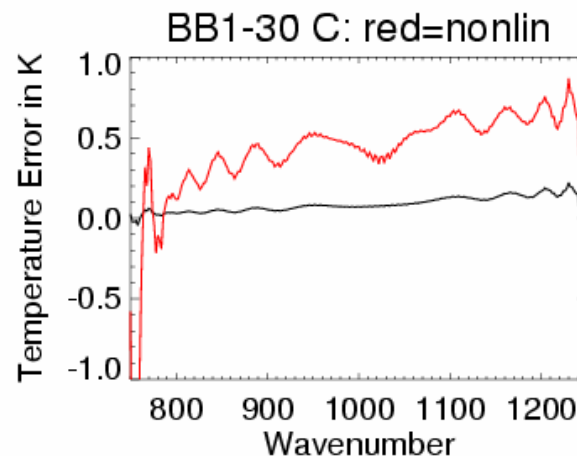
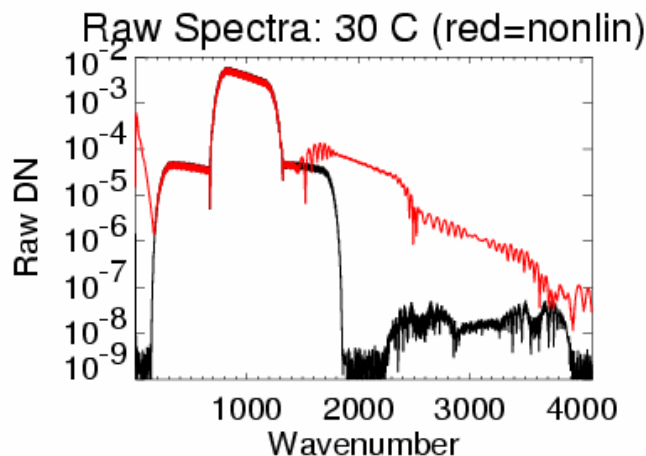
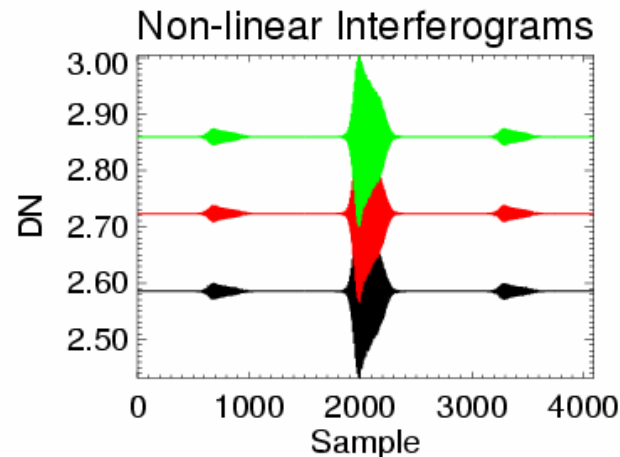
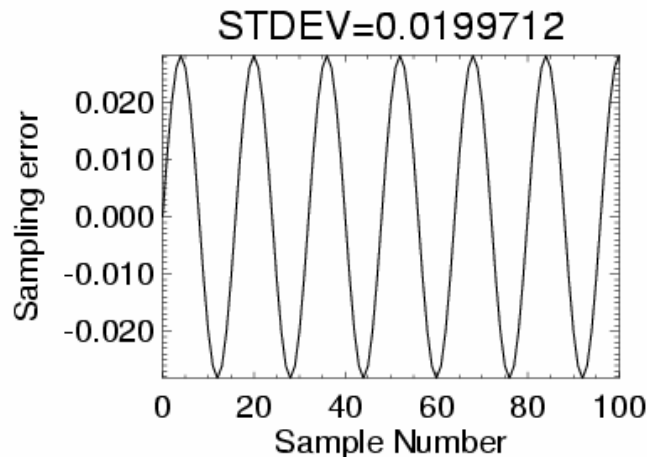


Non-linear + dispersion + channeling FTS



Non-uniform sampling + non-linear + dispersion + channeling FTS

Periodic sampling position error ΔZ and $SNR = \infty$: $\Delta Z(z) = a_0 \sin(2\pi \frac{z}{\delta z})$

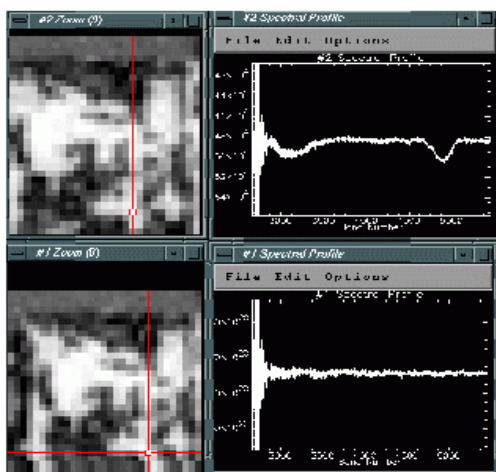


Effect of pointing jitter on FTS interferogram

Effect of jitter depends on the surrounding area:

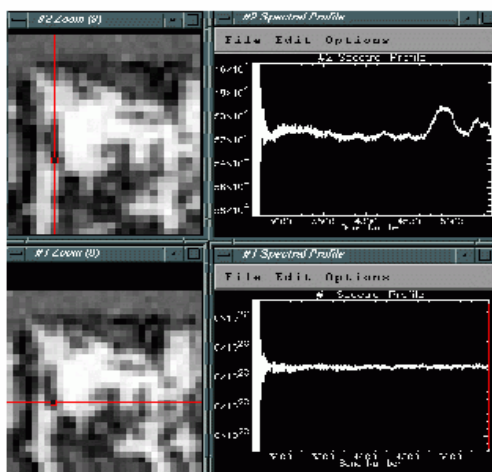
- A bright pixel surrounded by dark pixels shows strong base line shifts
- A dark pixel surrounded by bright pixels shows strong base line shifts
- A pixel in a uniform region shows no baseline shifts

Effect of Jitter Restoration on Pixels near Contrasts (a,b) and in uniform Regions (c) shown in the FTIR data cube



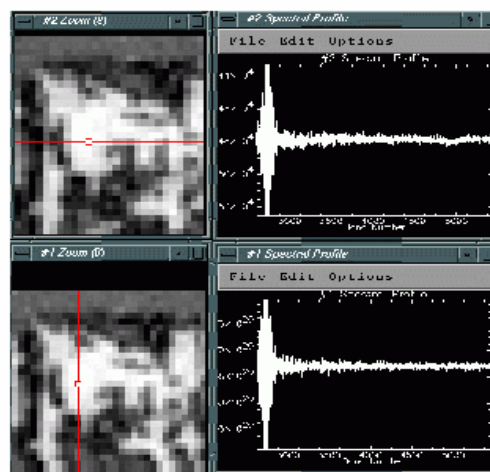
(a)

Bright Pixel



(b)

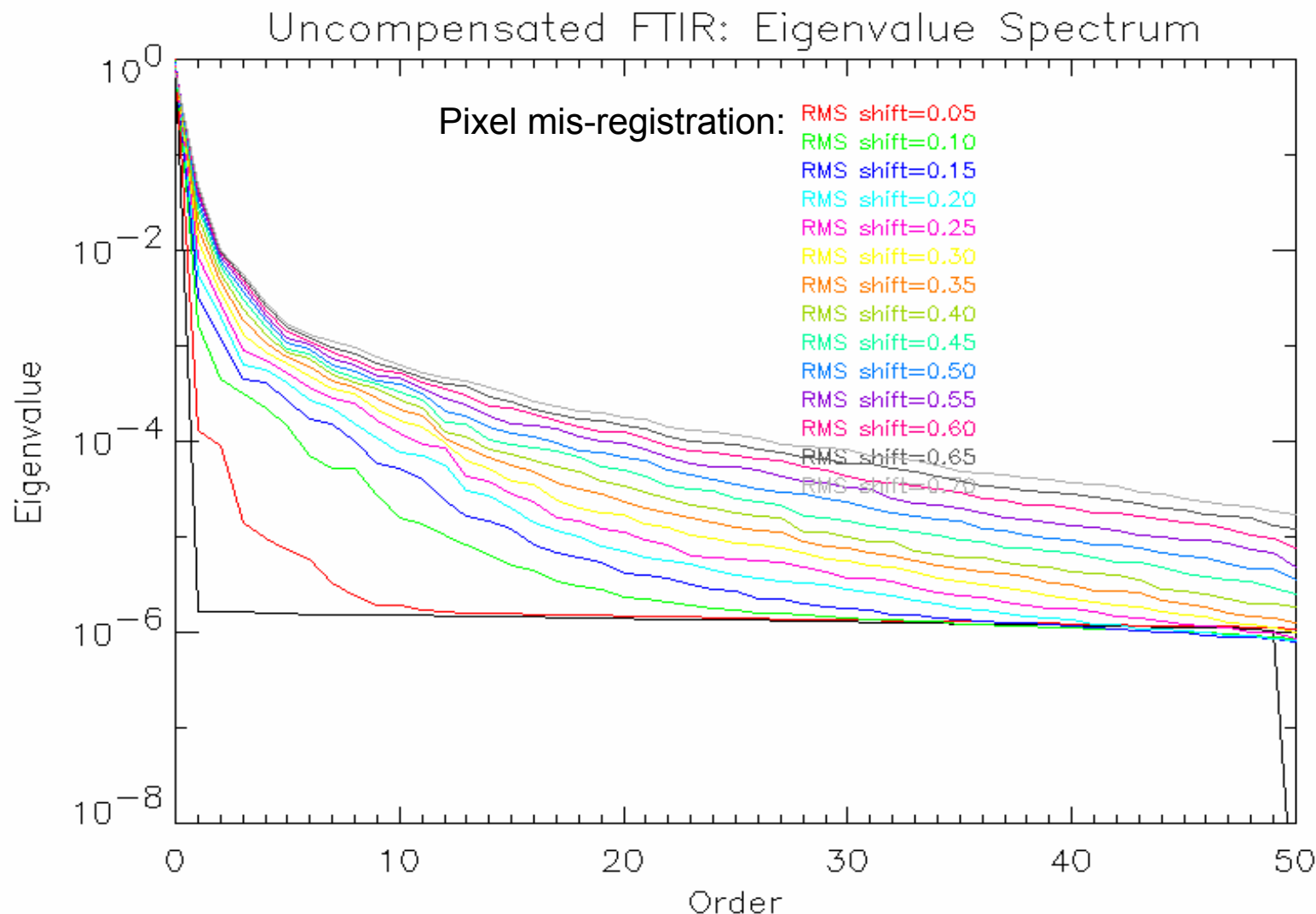
Dark Pixel



(c)

Uniform Pixel

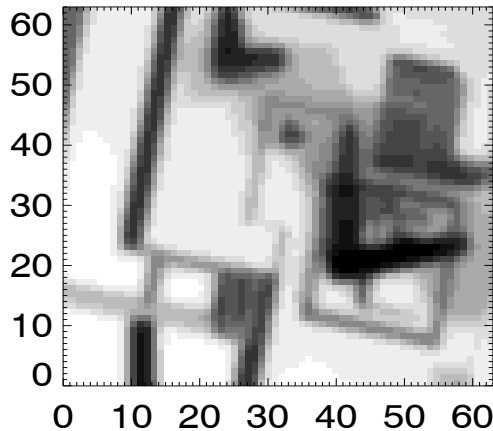
Effect of mis-registration on Eigenvalues in PC analysis



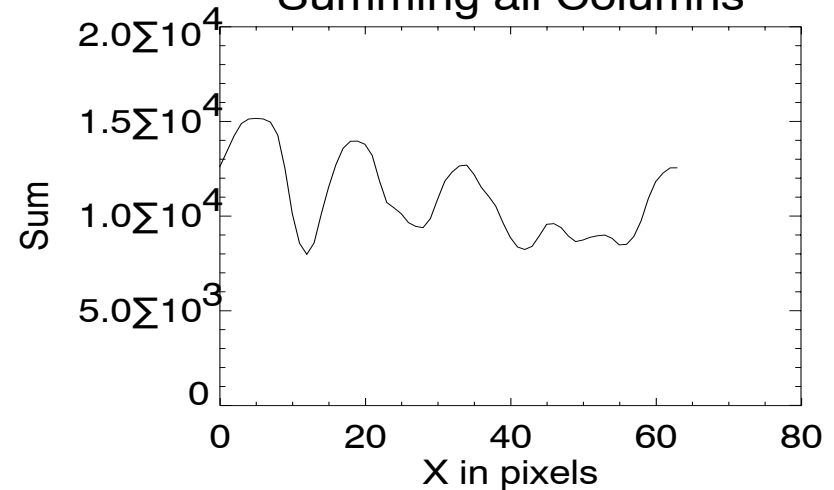
→ Information content seems to increase with mis-registration

1-D correction method for pointing jitter* (1)

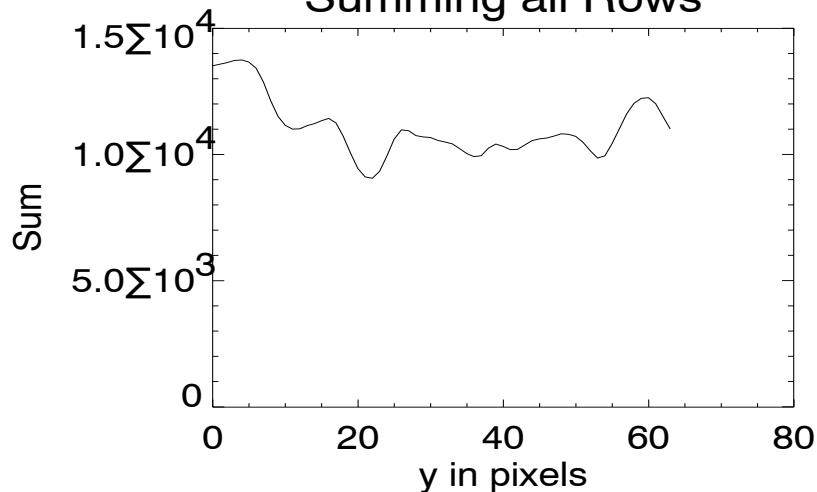
Window for Correlation



Summing all Columns

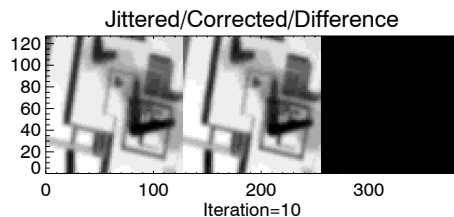
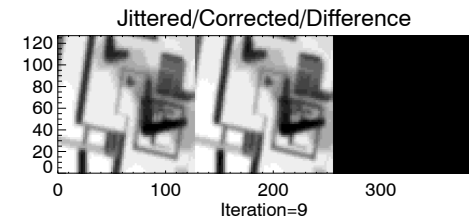
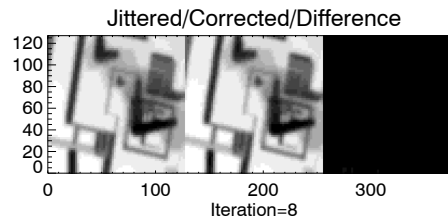
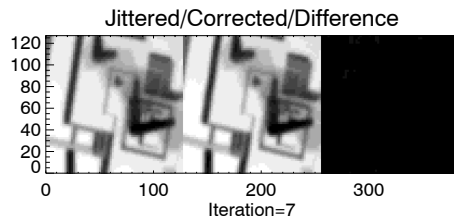
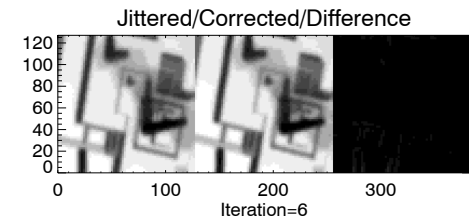
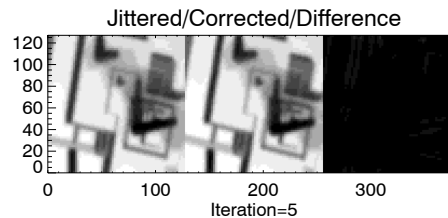
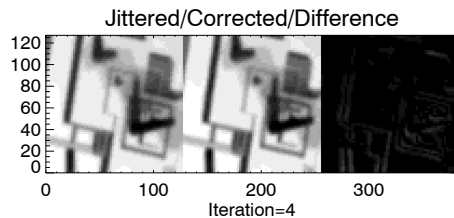
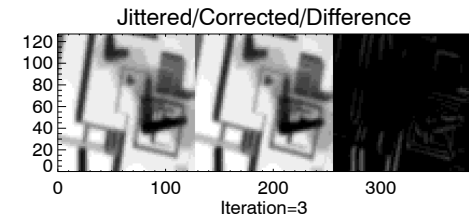
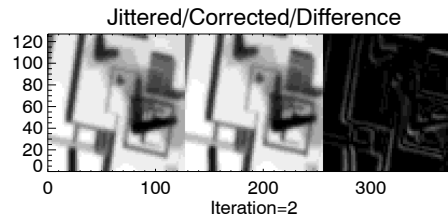
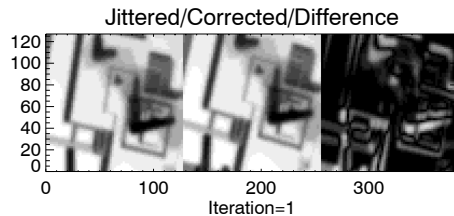


Summing all Rows



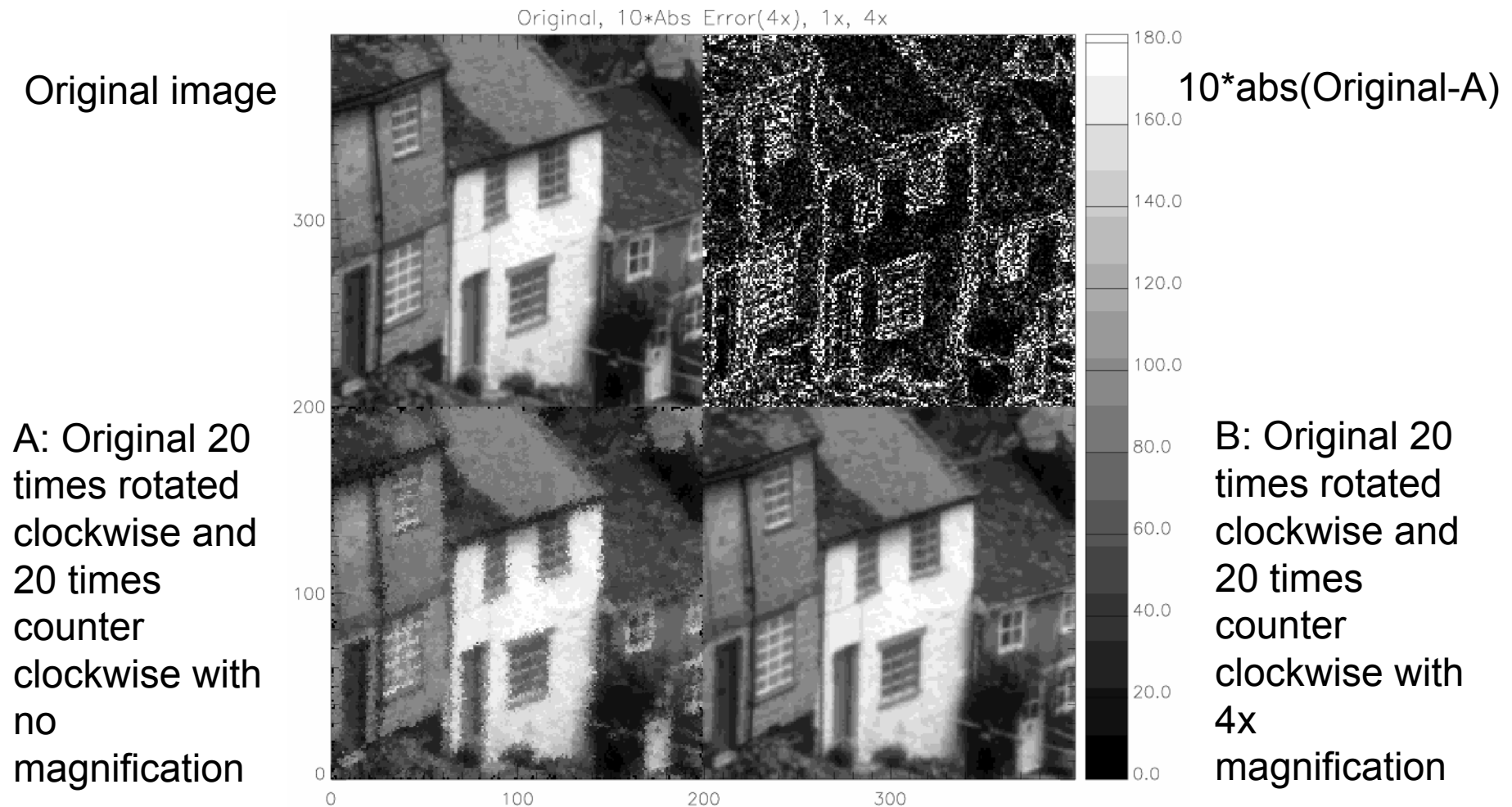
Sub-pixel tracking method sums up over all rows and columns of reference and to be correlated frames. The correlation is performed over two 1-dimensional arrays. Sub-pixel accuracy is achieved by cubic interpolation of the 1-D arrays.

Iterative correction of pointing jitter (2)



Iterative finding of x/y offset using the 1-D correlation method on simulated data.

Experiment: Effect of repeated resampling on imagery



→ Need to magnify image before resampling to minimize errors!

Correction of pointing jitter for a shaky video sequence (3)

Original
Image
Sequence



Translation
and rotation
corrected
pointing jitter

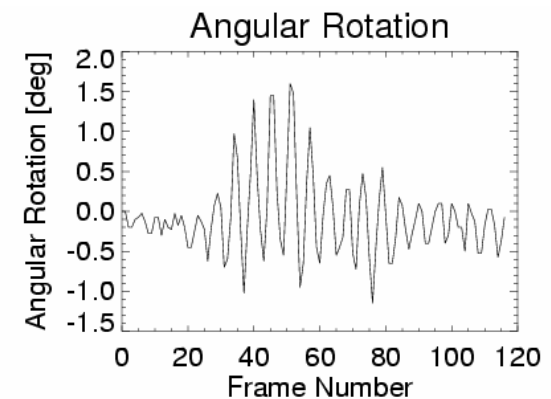
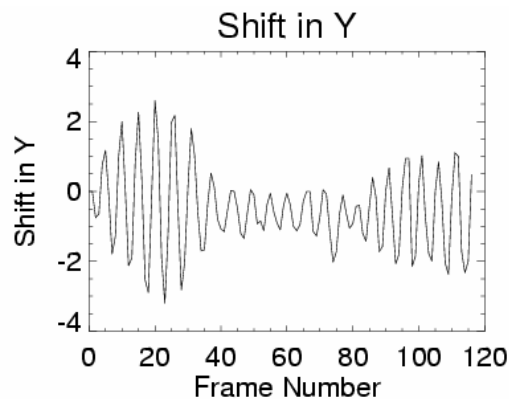
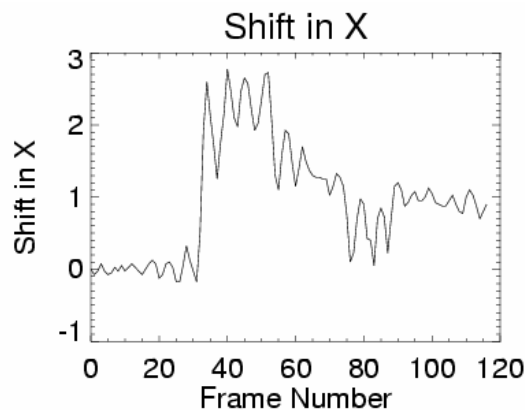
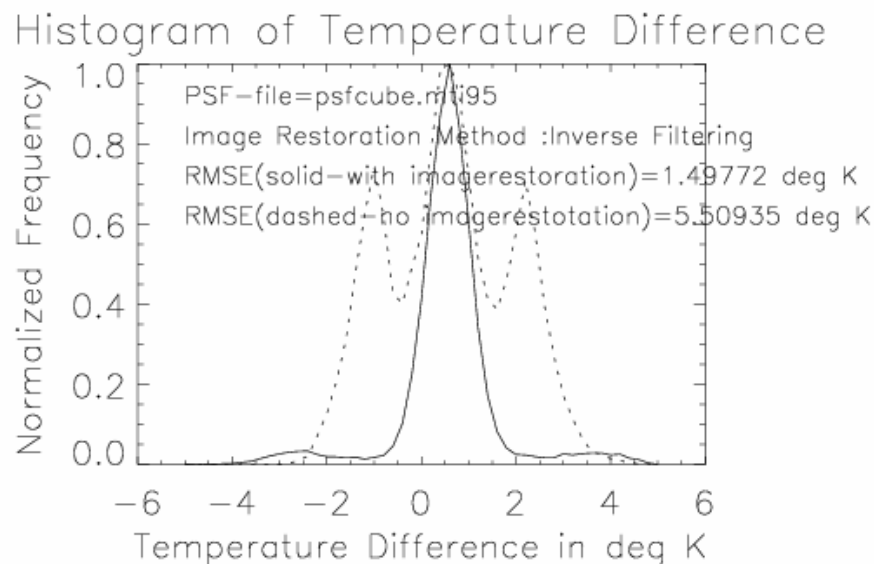
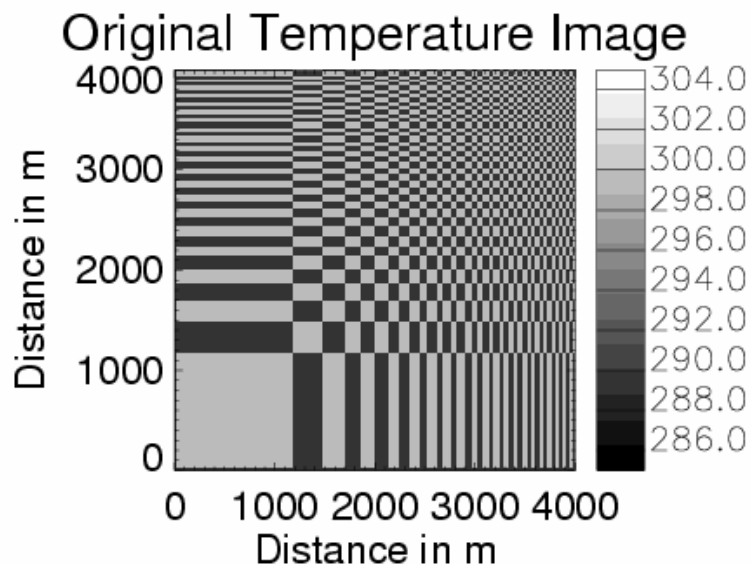
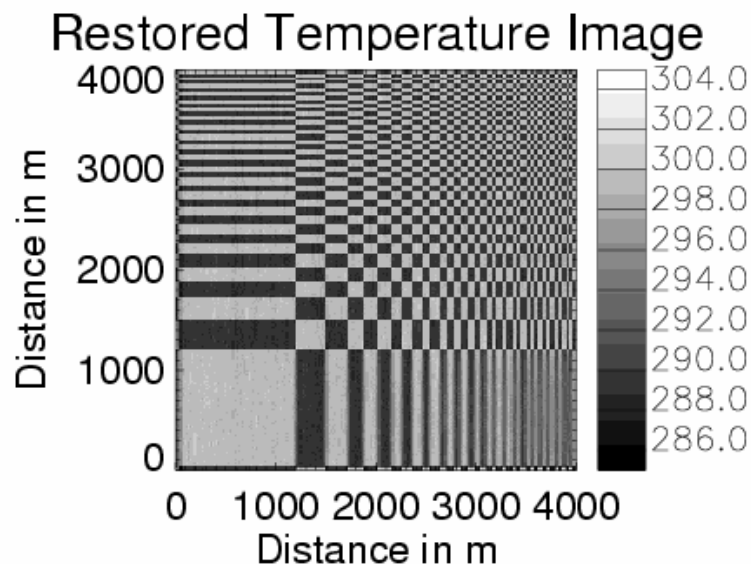
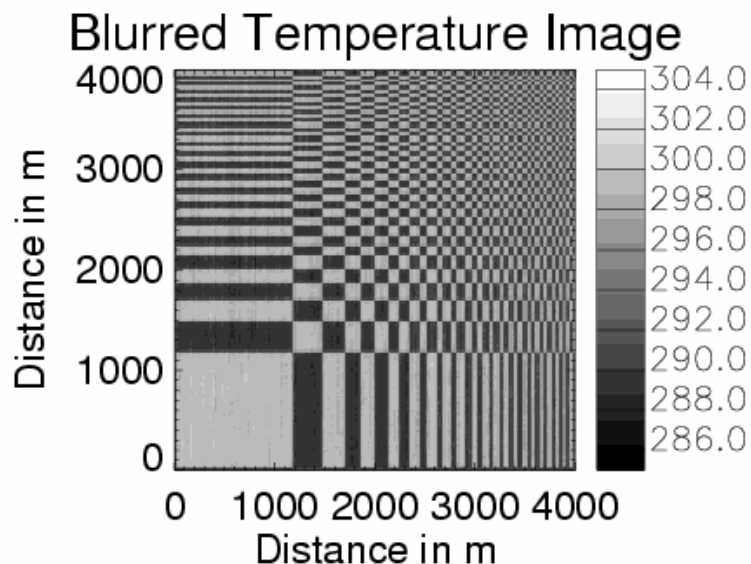


Image restoration decreases temperature retrieval error

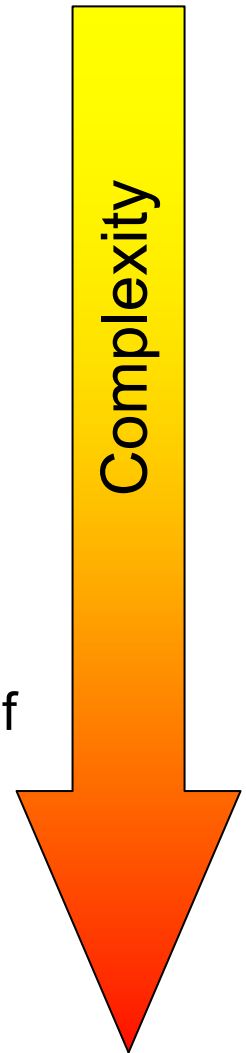


Mining of hyper-spectral information

- Hyperspectral data volume is large but contains correlated data (e.g. AVIRIS 224 bands contain up to 10 significant dimensions) → **need data compression!**
- Too simple assumptions of how to extract spectral information content can lead to errors (e.g. linear mixing and unmixing) → **need physically accurate modeling and non-linear retrieval methods**

Data compression algorithms

- Spectral compression by projecting data on orthogonal basis sets:
 - Principal components transform (KLT, Hotelling)
- Spatial compression using a frequency transform
 - Discrete Cosine Transform (e.g. JPEG)
 - Wavelet transform for spatial dimension (e.g. JPEG2000)
- Classification
 - K-means
 - Spectral angular mapping
- Spectral Unmixing
- Real-time atmospheric correction reduces dimensionality of data
 - express data in surface parameters (reflectance, emissivity, temperature) and atmospheric parameters (water vapor, ozone, visibility, temperature and relative humidity profile)
- Target detection and recognition



Linear spectral mixing theory*

- Measured reflectance in band i is:

$$\rho_i = \sum_{j=1}^N f_j \rho_{ij} + \varepsilon, \text{ where } \sum_{j=1}^N f_j \leq 1, \text{ where } i = 1, \dots, M$$

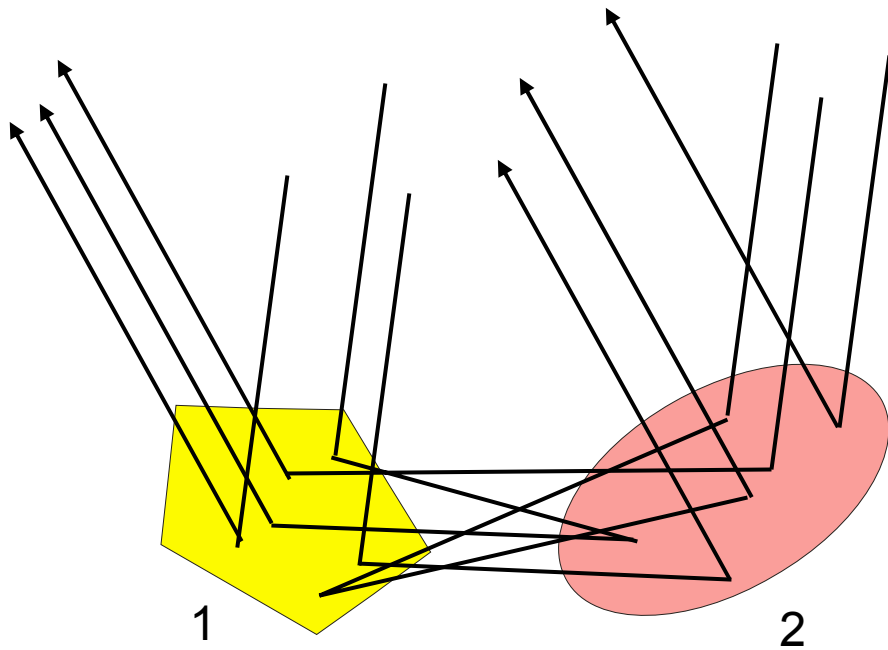
Pros & cons:

- + Model works when endmembers ρ_j are well defined
- + Makes sense for $N=2$ or 3 endmember mixtures
- It is hard to define useful endmembers at typical spatial resolutions of 20-30 m
- The assumption that reflectance ρ_i can be modeled as linear mixture of fractions f_j for a rough or structured 3-D surface is not valid when $\rho_j > 0.2$ or transparent surfaces are present (results in larger fitting error ε)

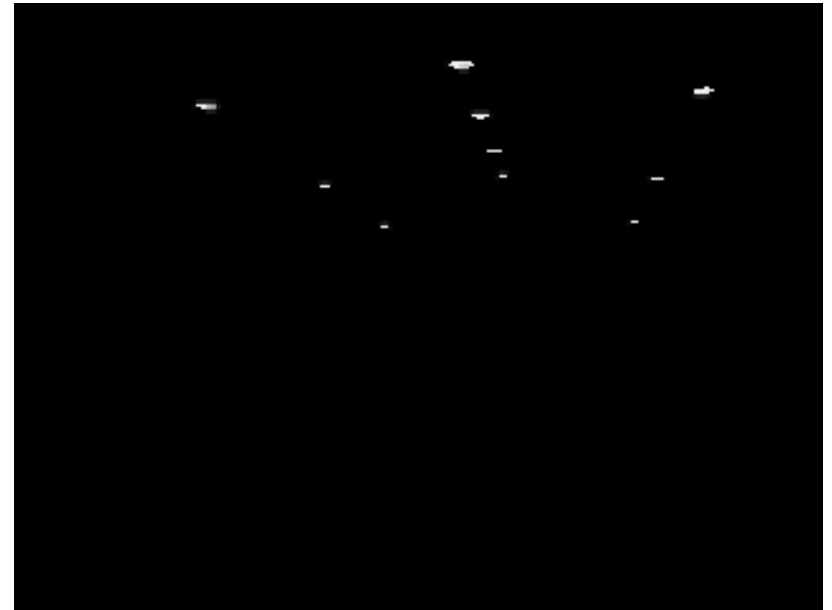
Non-linear spectral mixing theory*

- Reflectance is a nonlinear combination of reflectance spectra due to multiple scattering and transmission:

$$\rho = f_1\rho_1 + f_2\rho_2 + f_{12}\rho_1\rho_2 + f_{21}\rho_2\rho_1 + f_{121}\rho_1\rho_2\rho_1 + f_{212}\rho_2\rho_1\rho_2 + \dots$$

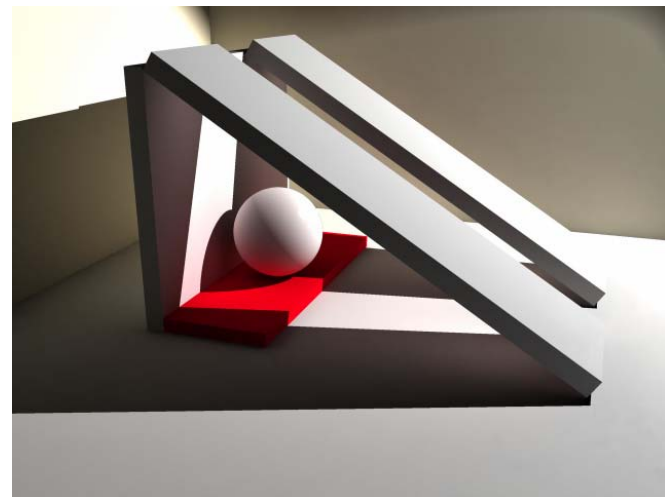
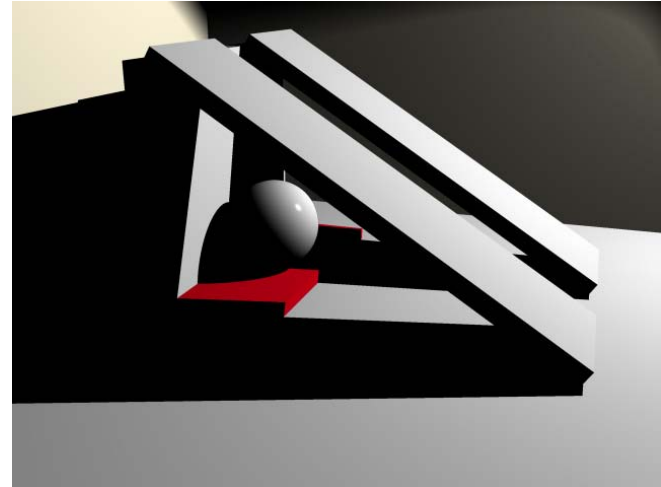


Movie of progressive radiosity

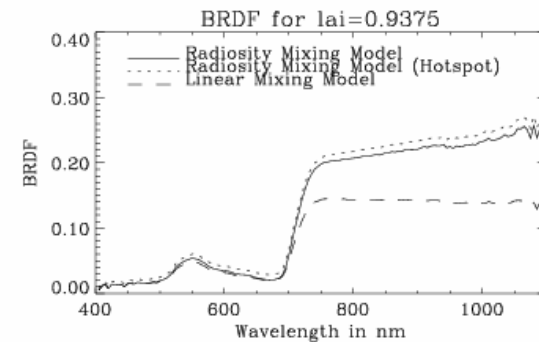
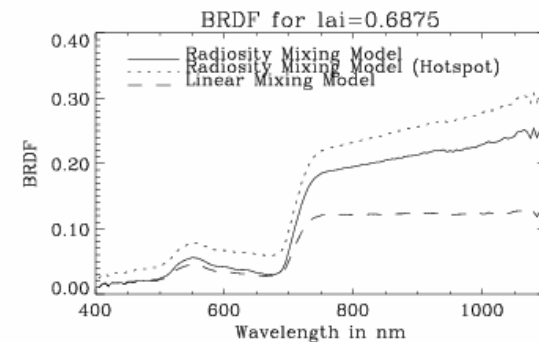
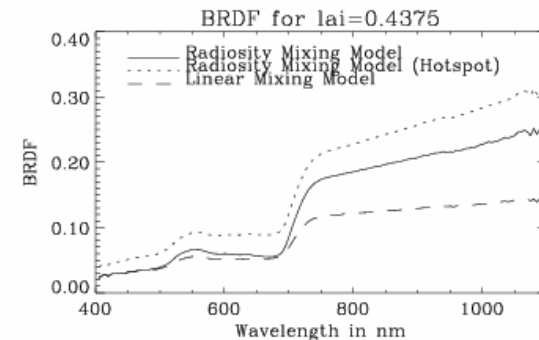
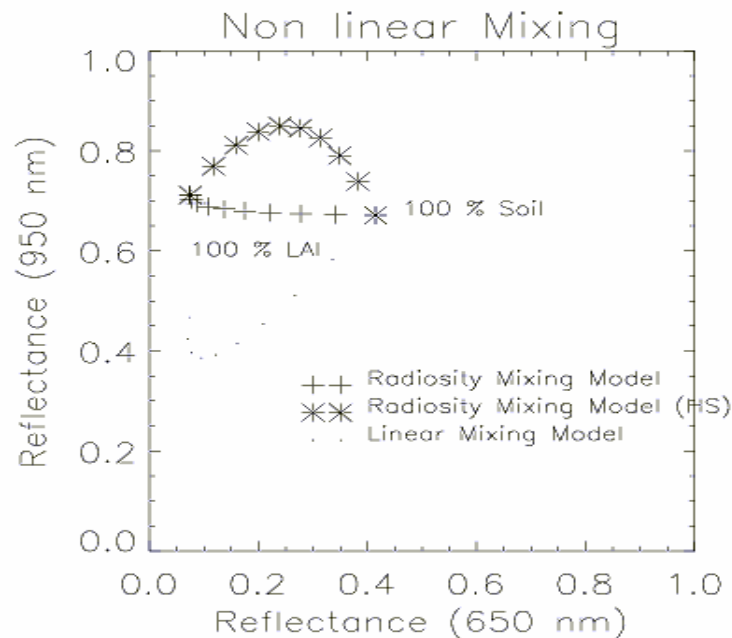
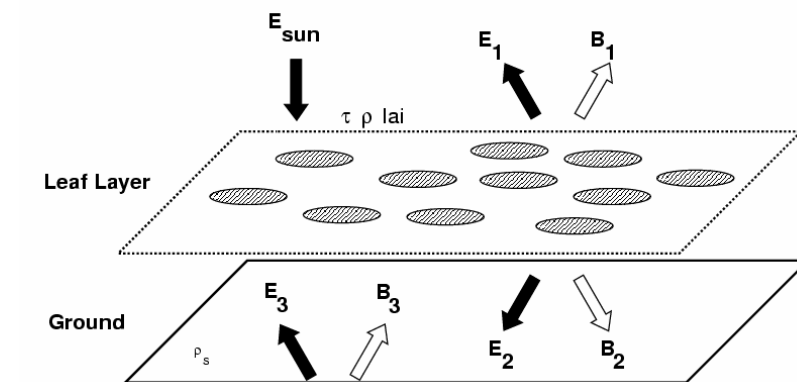


Visualization of linear vs nonlinear mixing

- Linear spectral mixing assumes there is only one interaction of a photon per surface → **raytracing**
- Nonlinear spectral mixing assumes there are many reflections between surfaces → **global illumination (radiosity)**



Simple example of linear vs nonlinear model



Conclusions



There are many challenges in the processing of hyperspectral imagery in the areas of:

- Atmospheric correction
- Sensor artifact correction
- Data exploitation

